

#3590 INSTITUTE OF PAPER CHEMISTRY
(Fiber Orientation Measurement)
Project Reports (1)

Institute of Paper Science and Technology
Central Files

MODELING MODERN PRESSURIZED PULP SCREENS

Douglas Wahren, IPC January 1986

In the design and operational optimization of screening and cleaning systems there is a need to model the actions of the components of the system on the components of the furnish being treated. It is shown below that one of the most commonly used concepts, characterization by means of the so called Q-value suggested by Bolton (1), although useful in many applications, has serious shortcomings when used for predictive purposes. Building on the pioneering work by Steenberg, Kubat, and Almin (2-7) and by Klemm (8) a very simple model of the screening process is proposed which appears to describe very well screening processes in modern industrial pulp screens operated at normal consistencies.

The model is based on the concept that there exists, for any given combination of particle type and screen arrangement, a single parameter, the passage probability (alternatively the retention probability), which uniquely describes the process. Over a range of operating parameters, e.g. flow rate, consistency, reject rate, etc., the passage probability remains constant. This approach enables predictive modeling of screening processes based on a minimum of experimental data.

It seems feasible to extend the validity of the model up into higher consistency regimes where particle interactions become important, but that is not the subject of this article.

The Basic Model for a Single Fraction

The essence of the present model builds on one basic assumption:

1. The screening behaviour of each defined fraction can be described by a single parameter, the passage (or retention) probability, i.e. each fraction behaves independently of other fractions.

The only application treated here is one where:

2. There is thorough mixing of the suspension on the feed side of the screen plate.

Assumption no. 2 limits the direct applications of the end results presented below to screen types where the incoming suspension is thoroughly agitated, but this is the case in most modern pressurized pulp screens. The case of

non-pressurized, "centrifugal" or "flat" screens, and other applications where successive dilution without back-mixing is used, might be treated as a finite or infinite series, a "cascade", of interconnected screens functioning according to both assumptions (4).

The notation used below is:

$M(x,y)$ = mass flow rate of fraction y in line x {kg/s}

$C(x,y)$ = concentration of fraction y in line x {kg/m³}

$Q(x)$ = volumetric flow rate in line x {m³/s}

$p(y)$ = net passage probability of fraction y , $0 < p < 1$

$n(y)$ = net retention probability of fraction y , $0 < n < 1$

$p(y) + n(y) = 1$

and in general:

$$M(x,y) = Q(x) * C(x,y) \dots\dots\dots(1)$$

$$C(x) = \sum_y C(x,y) \dots\dots\dots(2)$$

$$M(x) = C(x) * Q(x) \dots\dots\dots(3)$$

When used without the y -index, the symbols denote the total (of all fractions or of the single fraction being discussed).

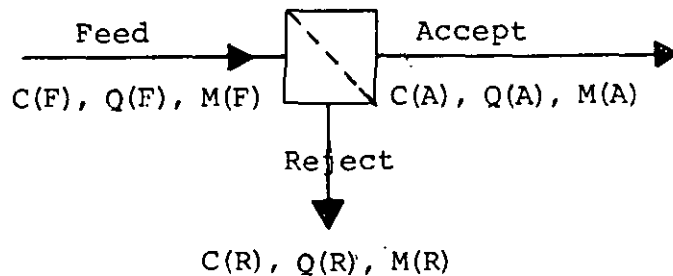


Figure 1. Screen symbol and notation used for consistencies volumetric and mass flows.

Referring to Figure 1, the three lines connected to the screen symbol are termed Feed, Accept, and Reject respectively, and indices F, A, and R are used to designate the lines. If dilution water is added it is considered to be part of the feed, i.e. part of $Q(F)$, and is not treated as a separate item in what follows.

Obviously:

$$Q(A) = Q(F) - Q(R) \dots\dots\dots(4)$$

$$M(A) = M(F) - M(R) \dots\dots\dots(5)$$

In real screens flows are externally controllable parameters. We therefore define the controllable, i.e. independent, variable R_v :

$$\text{Volumetric Reject Rate} = R_v = Q(R)/Q(F)$$

Conventionally, the reject rate is defined on a mass basis:

$$\text{Reject Rate (mass basis)} = R_m = M(R)/M(F)$$

Although often plotted and used as an independent variable (even in this article), R_m is, in fact, a variable which depends on many factors; it can be controlled only indirectly.

The key assumption of mixing is expressed in the diagram by noting that the consistency of the reject, $C(R)$, is the same as the consistency on the feed side of the screen plate. The other key assumption, number 1 above, is expressed by:

$$C(A,y) = p(y)*C(R,y) = \{1-n(y)\}*C(R,y) \dots\dots\dots(6)$$

In the special case of a single fraction this is just as well expressed by:

$$C(A) = p*C(R) \dots\dots\dots(6b)$$

Note that this assumption says nothing about the particular mechanism at work. If experiments show that p does indeed stay constant over some range of operating parameters then the model is validated over that range. Validation, obviously, involves measurement of accept and reject consistencies of one, two, or more fractions and determining p as the ratio between them. Experimentally this should be quite straightforward in most cases.

Note also, however, that both assumptions are perfectly compatible with, and in most cases identical to the statistical approach to screening developed and described by Steenberg and Kubat over 30 years ago (2,4-6) They also verified this approach thoroughly on a laboratory scale (7). They also showed (4,5) that, in theory, the parameter p or

$p(y)$ can take on values larger than one. So, the basic assumptions made here are not new but, rather, well proven in the laboratory but rarely applied or referred to today.

At the time Steenberg and Kubat published their work the numerical complexities involved in practical applications was a deterrent. Screens, generally, were not designed with mixing on the feed side, and instrumentation in screen rooms which would have helped verification efforts was lacking or non-existent. The situation today is markedly different in all respects. Notably, the detailed computations for a whole screenroom take up much less memory space in the personal computer than does the word processor used for writing this document. The equations can readily be integrated into larger systems modeling programs. It is time to revive a basically sound approach.

This approach is quite different in principle from the one leading to the use of Bolton's Q-value. The (implicit) assumption there is that the ratio of the shive content in the reject and accept flows is a function only of the reject ratio, R_m . As is discussed in a later section, this is not compatible with our assumptions except when the shive content is vanishingly small.

Referring again to figure 1 and equation 6b, it is obvious that the mass flow through the accept line can be written:

$$M(A) = Q(F)*C(F) - Q(R)*C(R) = \{Q(F) - Q(R)\} * C(R) * p \dots\dots\dots(7)$$

Inserting $Q(R) = R_v * Q(F)$ and $p = 1 - n$ yields:

$$C(R) = C(F) / \{1 - n * (1 - R_v)\} \dots\dots\dots(8)$$

$$M(A) = M(F) * (1 - n) * (1 - R_v) / \{1 - n * (1 - R_v)\} \dots\dots\dots(9)$$

$$R_m = M(R) / M(F) = R_v / \{1 - n * (1 - R_v)\} \dots\dots\dots(10)$$

These equations describe all essential conditions for the single-fraction case.

Multiple Components

As long as there is no interaction between the various components, or fractions, e.g. shives, fibers, fines, fillers, and grit, the relationships given above should hold for each fraction of a mixture. Obviously, there should be numerical differences between the passage probabilities for the various fractions.

Consider a mixture having j components being run at a volumetric reject rate of R_v . The reject rate on a mass basis for component i is:

$$R_m(i) = M(R, i)/M(F, i) \dots\dots\dots(11)$$

where

$$M(R, i) = \{M(F, i)*R_v\}/\{1-n(i)*(1-R_v)\} \dots\dots\dots(12)$$

and the total reject rate:

$$R_m = \sum_j M(R, i) / \sum_j M(F, i) \dots\dots\dots(13)$$

The consistency of the reject stream is:

$$C(R) = \sum_j C(F, i)/\{1-n(i)*(1-R_v)\} \dots\dots\dots(14a)$$

$$C(R) = \sum_j \{M(F, i)/Q(F)\}/\{1-n(i)*(1-R_v)\} \dots\dots\dots(14b)$$

The two forms of eq. 14 are identical in function but 14b is preferable when dilution water is used since it can be included in the term Q(F). The consistency of the accept stream is:

$$C(A) = \sum_j p(i)*C(R, i) \dots\dots\dots(15)$$

Designating fraction number \underline{s} as the undesirable component (\underline{s} for shives or stickies for example), the conventional measure of cleaning efficiency, \underline{E} is found:

$$E = M(R, s)/M(F, s) \dots\dots\dots(16)$$

where $M(R, s)$ is given by equation 12. The concept is readily extended to cover any number of undesirable components. The loss of desirable components, \underline{L} (\underline{L} for Loss), is given by:

$$L = \left\{ \sum_{i=1}^{s-1} M(R, i) \right\} / \left\{ \sum_{i=1}^{s-1} M(F, i) \right\} \dots\dots\dots(17)$$

Again, the concept is readily extended to any number, \underline{g} , of undesirable components simply by replacing the number $\underline{s}-1$ in eq. 17 by $\underline{s}-\underline{g}$.

Two Components: Shives and Fibers.

One of the ultimate objectives of this article is to indicate a practical way of dealing with multiple components, e.g. shives, fibers, fines, and fillers in screening operations. Methods for doing that are indicated above. The two-component case is the simplest one which has any

practical significance, and it is also one which has been extensively treated in the literature, thus providing the opportunity for comparisons to previous work. This special case is therefore treated rather extensively.

The two components are usually a desirable and an undesirable fraction and the objective is to remove as much as possible of the undesirable component with as little loss of the desirable component as possible. In the following the desirable component is termed f , or fibers, and the undesirable component is termed s or shives. These designations are selected to serve as mnemonics; the two fractions could be any two collections of components of interest. By definition then, in what follows, anything which is not a "shive" is considered to be a "fiber".

For this part of the analysis the mass flow to the screen is normalized:

$$M(F,f) + M(F,s) = 1 \dots\dots\dots(18)$$

Hence, in order to obtain actual mass and volumetric flow rates the values computed by the various formulas should be multiplied by the actual mass flow rate into the screen. It follows directly from eq. 12 that the mass flows of fibers and shives to the reject are:

$$M(R,f) = \{M(F,f)*R_v\}/\{1-n(f)*(1-R_v)\} \dots\dots\dots(19)$$

$$M(R,s) = \{M(F,s)*R_v\}/\{1-n(s)*(1-R_v)\} \dots\dots\dots(20)$$

Equation 16 lists the conventional measure of cleaning efficiency which here translates into:

$$E = R_v/\{1-n(s)*(1-R_v)\} \dots\dots\dots(21)$$

The shive content of any flow is defined as the ratio of the mass of shives to the total mass of shives plus fibers.

Hence, for any flow, x , the shive content is:

$$S(x) = M(x,s)/\{M(x,s)+M(x,f)\} \dots\dots\dots(22)$$

Using eq. 13 for the two-component case, and $S(F)$ to designate the shive content of the feed, the reject rate on a mass basis is readily found:

$$R_m = \{S(F)*R_v\}/\{1-n(s)*(1-R_v)\} + \{(1-S(F))*R_v\}/\{1-n(f)*(1-R_v)\} \dots\dots\dots(23)$$

Equations 14 and 15 give the consistencies of the reject and accept flows:

$$C(R)/C(F) = S(F)/\{1-n(s)*(1-R_v)\} + \{1-S(F)\}/\{1-n(f)*(1-R_v)\} \dots(24)$$

$$C(A)/C(F) = p(s)*S(R)*C(R) + p(f)*\{1-S(R)\}*C(R) \dots(25)$$

Equation 12 or 17 gives the loss of fibers as a fraction of the fiber stream fed to the screen:

$$L = R_v/\{1-n(f)*(1-R_v)\} \dots\dots\dots(26)$$

Note that, as would be expected from the assumption of non-interaction, the shive content of the feed has no influence on the fiber loss when using the volumetric reject rate as a basis. Writing the fiber loss as a function of the reject rate on a mass flow basis is readily done but yields an unwieldy formula involving, among other variables, the shive content of the feed. Such a relationship is illustrated in Figure 2. The simplicity of eq. 26 and related equations is one of the good features of the present approach -- including the use of the volumetric reject rate as an independent parameter.

Figure 2 illustrates both the shive removal efficiency and the fiber loss as functions of the total reject rate, R_m . Parameter is the shive content, $S(F)$, in the feed stream. Notice that the shape of the curves changes with the shive content.

Eliminating R_v between eq's 21 and 26 and using the passage probability, $p(y)=1-n(y)$, it is readily shown that the fiber loss and the screening efficiency are related by:

$$1/L = 1 + \{p(f)/p(s)\}*\{1/E-1\} \dots\dots\dots(27)$$

Hence, the ratio of the passage probabilities for fibers and shives is the sole design parameter linking fiber loss to screening efficiency. This important ratio is readily evaluated from coherent experimental data of E and L :

$$p(s)/p(f) = (1/E-1)/(1/L-1) \dots\dots\dots(28)$$

This concept can be extended, and it can be shown for any number of components, i, j, \dots , that the ratio $p(i)/p(j)$ uniquely determines $E(i)$ as a function of $L(j)$ or as function of the sum of the loss of any number of fractions, l, k, \dots . Hence, a diagram of, say, shive removal efficiency as a function of reject rate remains unchanged if the passage probabilities of all the components of the furnish (shives, long fibers, short fibers, and fines for instance) are multiplied by the same factor. What does change is the thickening of the reject stream and the thinning of the accept stream.

Three Components: Shives, Long Fibers, and Fibers.

In many practical applications, such as TMP screening, a minimum of three components must be considered. To facilitate readability they are here termed Shives (undesirable), Long Fibers (very desirable) and Fibers (anything that is not Shives nor Long Fibers). We may define a "Long-Fiber Loss", LL , as:

$$LL = M(R,L)/M(F,L) \dots\dots\dots(17b)$$

and make use of equations 1-17 to define this case. Some results are exemplified in Figure 2, where all curves show the shive removal efficiency, E , as a function of the reject rate. All the curves have been calculated and plotted using the following passage probabilities:

Shives: 2%
 Long Fibers: 10%
 Fibers: 50%

The difference between the curves is in the composition of the furnish:

	Shives	Long Fibers	Fibers
A:	1%	0	99%
B:	30%	0	70%
C:	70%	0	30%
D:	1%	80%	19%

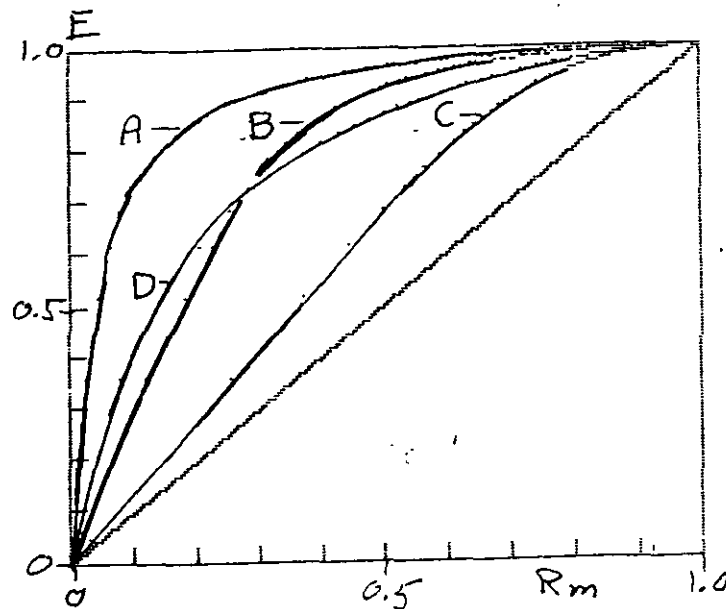


Figure 2. Shive removal efficiency as a function of reject rate. Four different compositions were used in this hypothetical example. Passage probabilities and furnish composition are given in the tables above.

All the curves essentially illustrate two-component cases; A, B, and C show the progressive influence on the curve shape and location of a high shive content, and curve D the influence of a long-fiber fraction. Please note that only curve A would be accurately described by a Q-value according to Bolton ($Q=1-0.02/0.50=0.96$) as discussed below.

Bolton's Q.

The Q-value, defined by Nelson (1) but referred to Joseph A. Bolton, is commonly used to characterize the cleaning efficiency of screens and cleaners. Bolton's Q-value deals only with two-component systems comprised, for instance, of fibers and shives. It is defined to relate, in a simple manner, the cleaning efficiency, E , to the reject rate, R_m . In our notation:

$$E = R_m / \{1 - Q * (1 - R_m)\} \dots\dots\dots (29a)$$

$$E = R_v / \{1 - n(s) * (1 - R_v)\} \dots\dots\dots (29b)$$

The first version defines the Q-value. A single parameter, Q , describes the entire conventional screening efficiency curve. When Q is zero there is no cleaning effect and when Q approaches one the cleaning efficiency approaches the ideal, i.e. 100% removal of shives at a vanishingly small reject rate. This is a very useful concept when dealing with screening and cleaning operations where the shive content is small.

The second version of eq. 29 is included to show the analogy between the Q-value and the retention probability for shives. The main difference is that the retention probability deals with volumetric flow rates whereas the Q-value deals with mass flow rates.

In eq. 29a solving for Q yields:

$$Q = \{E - R_m\} / \{E * (1 - R_m)\} \dots\dots\dots (30)$$

Assuming that the shive content of the feed is very small, i.e. that $S(F)=0$, and inserting E and R_v from equations 21 and 23 respectively, one finds that the Q-value for zero shive content is:

$$Q_0 = 1 - p(s)/p(f) \dots\dots\dots (31)$$

Using eq. 27 the above relationship also uniquely defines the fiber loss in this case:

$$1/L_0 = 1 / \{(1 - Q_0) * (1/E - 1)\} - 1 \dots\dots\dots (32)$$

These relationships are good approximations of real situations where the shive content is only a few percent by

mass; this would cover many primary screening and cleaning operations. When considering the "recovery" (or reject handling) part of a screening or cleaning system, however, the shive content can be quite high and the Q-value cannot be considered a constant. This is demonstrated in Figure 3, where the Q-value is shown as a function of the reject rate, R_m , for a two-component system comprised of fibers and shives in various proportions.

The passage probability of the shives is 5 percent and the passage probability of the fibers is 90 percent. The Q-value is plotted as a function of the reject rate, R_m , for shive contents from zero to 99 percent. At zero shive content the Q-value is a true constant having the value of $1-(5/90)=0.944$ but at other shive contents the value of Q varies widely and approaches zero as the shive content approaches 100 percent.

In a three-component system, e.g. one containing shives, long fibers, and fibers as exemplified in figure 2, the Q-value is also influenced by the the long-fiber content but to a much lesser extent.

Hence, the Q-value is not a characteristic of the screen-and-shive characteristics but varies with furnish composition and operating parameters as well. So, although mathematically convenient, Q is not a constant nor a characteristic, at least not if the passage probability for each fraction is a constant.

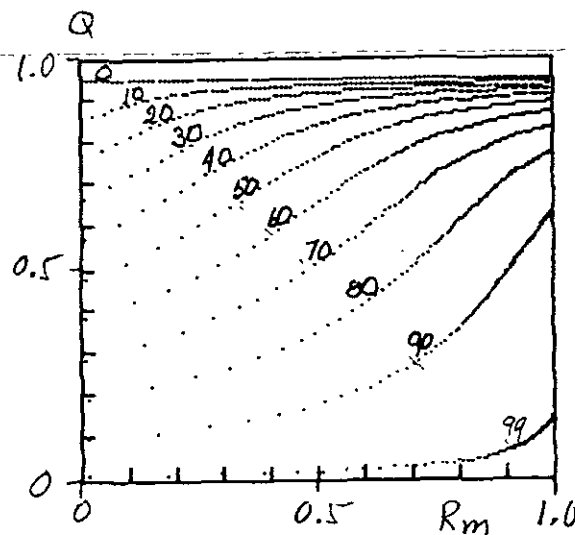


Figure 3. Bolton's Q value as a function of reject rate in a hypothetical case where the shive content is varied from 0 to 99%. The passage probability of the shives is 5% and of the fibers, 90%.

Fredriksson's T

In many applications, particularly those dealing with TMP and CTMP pulps, screens and cleaners have a very noticeable fractionating effect. Valuable long fibers may become part of the reject stream to a much higher degree than do the short fibers. In the present context, the passage probability of the long fiber fraction is substantially less than the passage probability of the rest of the fibers. This can be considered to be a three-component case which is readily handled by equations 11-17.

Realizing the importance of this three-component case Fredriksson (9) defined a parameter, T , which in our notation is:

$$T = (1/LL-1)/(1/Rm-1) \dots\dots\dots(33)$$

where LL is the fraction of the Long fibers "Lost" to the reject. Fredriksson's T -value is a close kin of Bolton's Q -value. This can be demonstrated by defining $To=1-T$. Insertion into eq. 33 and re-arranging gives:

$$LL = Rm/\{1-To*(1-Rm)\} \dots\dots\dots(34)$$

Compare this expression to eq. 29 and the relationship is obvious. Unfortunately, therefore, Fredriksson's T -value suffers the same shortcoming as Bolton's Q -value in that it too depends on the shive content of the feed and on the long-fiber content.

This is demonstrated in Figure 4 which shows T as a function of the reject rate, Rm . The passage probabilities are the same as used in figure 3, i.e. the passage probability is 2 percent for shives, 10 percent for long fibers, and 50 percent for fibers.

Figure 4a shows the influence on T of the shive content and Figure 4b shows the influence on T of the long-fiber content. Only in the case of zero shive content and zero or 100 percent long-fiber content does the value of T stay a true constant characteristic of the performance of the screen.

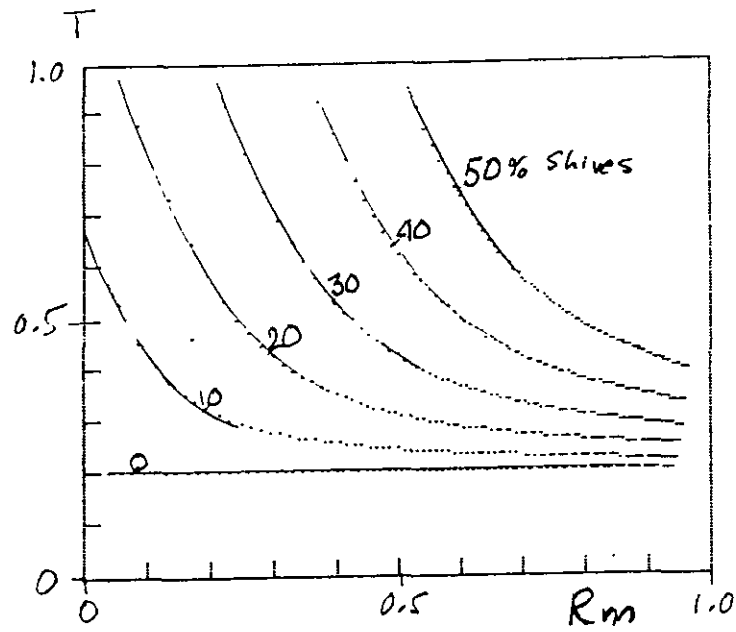


Figure 4a. Fredriksson's T as a function of reject rate in a hypothetical case where the shive content has been varied from 0 to 50%.

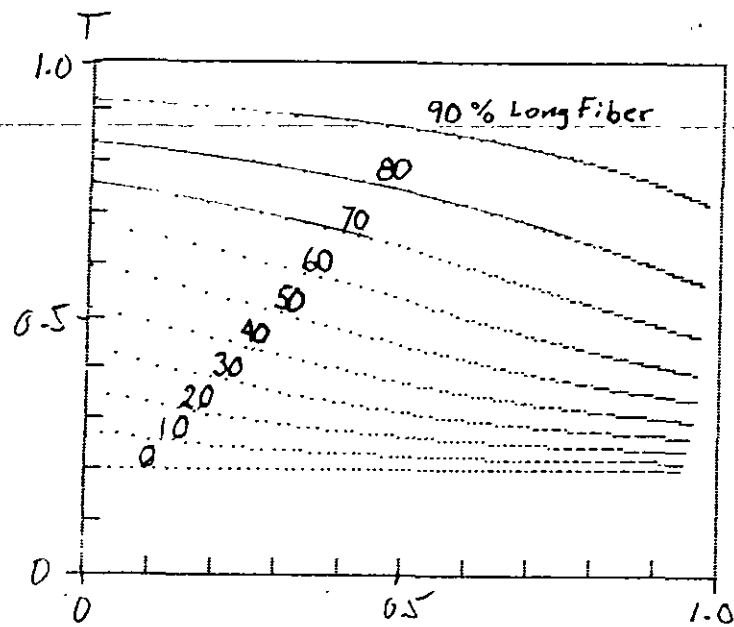


Figure 4b. Fredriksson's T as a function of reject rate in a hypothetical case where the long-fiber content has been varied from 0 to 90%.

Partial Verification using Mill Data.

Kubat, one of the originators of the basic concept set forth here, verified experimentally the constancy of the passage probability of various fractions (7) and also demonstrated the validity of the model of particle interaction at higher consistencies proposed by him (6). His experiments, however, were limited to a very small scale laboratory vibrating screen.

It is clearly desirable to verify any theory or model of this kind in actual mill-scale operation. Considerable difficulties are usually encountered when attempting to validate any theory through mill-scale experiments. The approach presented here offers a simple means for verification of the model and for providing quantitative data from any installation where reject and accept flows can be sampled. According to eq. 6, the passage probability, $p(y)$, for any fraction, y , is simply measured as the ratio of the consistencies of that fraction in the accepts and rejects.

In most real screens, however, dilution water is added in such a way as to do the maximum good with a minimum of addition. This often involves splitting the dilution water between the feed and the reject sides of the screen. This is done empirically based on two criteria; to keep the rejects fluid enough and to minimize the loss of good fiber, but the split ratio is rarely known. The reject consistency, therefore, has little relevance for a spot check on passage probabilities using eq.6. A more useful version is found by simple substitution:

$$p(y) = 1/\{1+[C(F,y)/C(A,y)]/Rv\} \dots\dots\dots(34)$$

The accept and feed consistencies, in toto or concerning any component of them, are influenced to a much smaller degree by the dilution water than is the reject consistency because the the flow rates are high compared to that of the dilution water.

To complicate matters further, whitewater -- not fresh water -- is used for dilution, and its content of any fraction of interest must be taken into account. For serious mill-scale work, therefore, it is necessary to make complete mass balances for all flows and fractions of interest. Fortunately, that is precisely what Borje Fredriksson did (9). I am indebted to him and to SCA (Svenska Cellulosa Aktiebolaget) for permission to review some of the raw data used as a basis for his article.

Without going into detail it can be stated that the data do not refute the basic assumptions made here over the ranges tested. Some of the ranges are very narrow, however. The shive content of the feed varied only between 1.5 and 3

percent and the long-fiber content only between 45 and 48 percent. Reject rates, R_m , were varied between 15 and 40 percent and the feed flows were varied quite widely. So, there is much more work to be done, but at least we have some indications of validity on a real, mill-scale basis. Student work at IPC, planned for execution in 1986, is aimed at obtaining further data.

The machines reported on here are the same as were reported on by Fredriksson (9). They are:

- A. Centrisorter with 0.4 mm slots - TMP
- B. Centrisorter with 1.4 mm holes - TMP
- C. Centricleaner, 6" diameter - CTMP

The fractions studied in each case were:

Shives: Sommerville, retained on 0.15 mm screen plate
 Long Fiber: Bauer McNett, retained on 30 mesh screen
 Fiber: All solids except shives and long fibers

All data obtained on screen A under various operating conditions and evaluated in different ways are displayed in Figure 5. The shive removal efficiency is shown as a function of the reject rate, R_m , and of the long-fiber loss, LL . Data obtained in a mill environment are subject to errors and variations of many different kinds, notably composition of the furnish between tests, flow rate variations and inaccuracies of their measurements, the split of dilution water, etc. Obtaining truly representative samples with a minimum of fractionation due to sampling is another significant problem in this particular context. Other sources of error include testing of shive and long-fiber content.

It is tempting therefore to resort to data reconciliation by some standard method, but in order to give an impression of the high quality of Fredriksson's data all measured data points concerning screen A were used to produce the diagram shown in Figure 5. Each operating condition was evaluated in four different ways from measurements on feeds, accepts, and rejects and using widely different assumptions concerning the split of dilution water. Using the equations for the three-component case, corrections of the feed composition were made to a constant shive content of 1.5 percent and constant long-fiber content of 45 percent. Evaluated in this way the resulting data represent the widest possible spread, or maximum uncertainty. Still, all the data fall within the shaded areas of the two curves.

A curious observation should be mentioned. In a fairly large number of cases studied, and particularly those using drilled screen plates with a large open area, the partial concentration of fibers in the accept stream was higher than

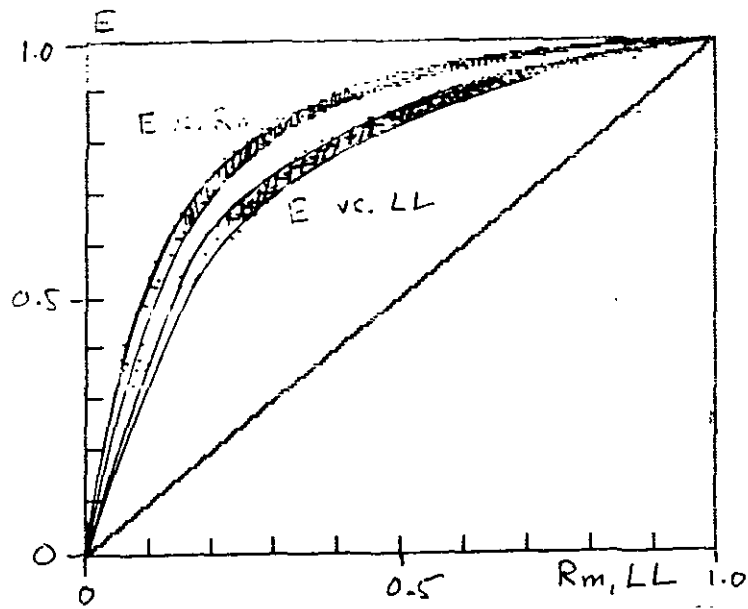


Figure 5. Shive removal efficiency as a function of reject rate and long fiber loss. The crosshatched area contains all individual data points evaluated by various means for Screen A and compensated to shive content of 1.5% for a long-fiber content of 45%.

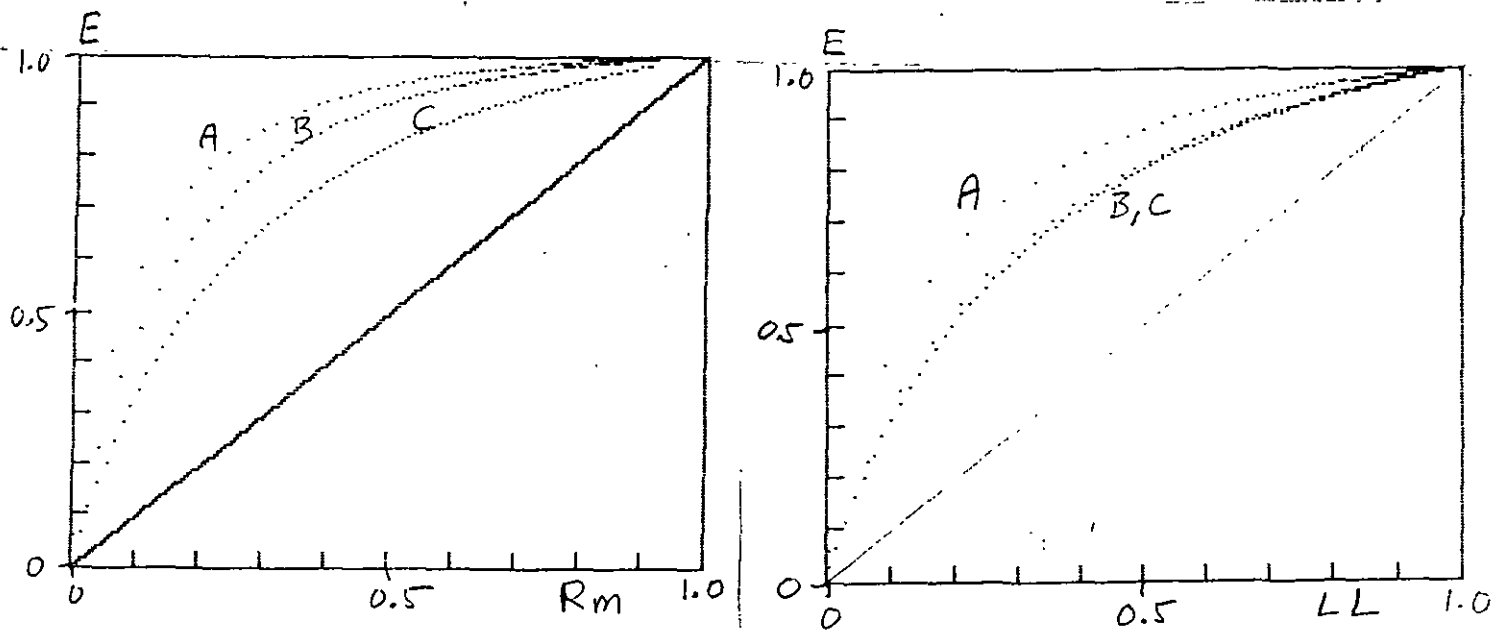


Figure 6. Diagram A, on the left, shows the shive removal efficiency as a function of reject rate for Screens A, B and C. Diagram B, on the right, shows the shive removal efficiency as a function of the long-fiber loss for the same machine.

in the feed! Note that Fredriksson's experiments were not designed to give direct information on this particular issue, so this observation relies on relatively small differences between large numbers. It does not take large analytical errors in the Bauer-McNett classification for instance to cause such apparent discrepancies even if the fiber concentration in the accept stream is just slightly lower than in the feed.

There is a possibility, however, that these effects are real. Kubat and Steenberg (4) showed theoretically that, in the presence of large pulsations across the screen plate, there is a possibility that the "permeability index" may be higher than one. As far as I know this has not been experimentally demonstrated, and the present data do not allow any conclusions to be drawn in this respect. It should be noted that with a large long-fiber fraction in the furnish, such as was the case in the experiments reported here, the data on the passage probability of what is here termed the fiber fraction are the least reliable.

As it turns out, when using eq. 34 for the evaluation of passage probabilities, any reasonable assumptions made concerning the split of the dilution water yield virtually identical (coefficient of variation no higher than 2.5 percent!) probability ratios and, therefore, identical curves in the diagram. The only remaining uncertainty then concerns the absolute levels. That uncertainty is of the order of 5 percent of the values given in the following table.

The uncertainties associated with use of data obtained from the reject stream are higher and are the main contributors to the spread shown in Figure 5. These data points were disregarded in the following.

As it turns out, all the results can be expressed, within the accuracy of the measurements, by the following passage probabilities:

Fraction	Machine:		
	A	B	C
Shives:	1.52	3.67	16.5
Long Fiber:	11.1	15.8	65.9
Fiber:	56.0	82.2	90.1

Table of passage probabilities, expressed as percentages, for some fractions screened by three different machines.

The resulting diagrams, machine generated using the three-component model and the above data, are shown in Figure 6. Figure 6a shows the screening efficiency, \bar{E} , as a function of the reject rate and figure 6b shows the screening efficiency as a function of the long-fiber loss, \underline{L} . All

curves are virtually identical to those shown by Fredriksson (9) and therefore convey no new information per se.

The difference is that, if the model holds, the data could be used even if the proportions of the components were to be changed significantly. As exemplified in figure 2, it is possible to calculate, for instance, the behaviour of each fraction in the reject screening part of the system where the shive content is high. Melding these concepts into a computer model of the whole system would take all effects into account. It would become possible to optimize system performance based on simple passage probabilities, such ^{as} those listed in the table, and user-imposed criteria for optimum performance. Such predictive use of experimental information is not possible using concepts like Q and T values.

Conclusions

Characterizing the performance of screening operations by means of passage probabilities which remain constant for each defined fraction, is compatible with the approach using Bolton's Q and/or Fredriksson's T only when all fractions except one are very small.

As far as it can be demonstrated experimentally that the passage probabilities of various fractions remain constant, the present approach should facilitate accurate predictive modeling of screening systems using any number of fractions and any composition of the feed to each screening unit.

Evaluation of the parameters of the present model only involves measurements of the concentration of each fraction of interest in feed and accept flows over a desired range of operating parameters (flow rates, reject rates, feed consistencies, etc.). Although it is necessary to watch out for influence of extraneous factors, such as local dilution with whitewater, it is no more complicated to make such evaluations in a mill environment using this model than using the more common approaches.

Partial validation of the model has been obtained from the literature and other sources but each application requires quantification over some operating range. The advantage of the approach presented here over other methods is that experimental data should be more readily transferable to new or extended applications. It is postulated that, as the body of knowledge of passage probabilities grows, it may become possible to predict such quantities based on characteristics of the screening machine, notably the design of the screen plate, and hence, to design from theory and systematized data entire screening and cleaning systems to meet specific performance criteria.

There probably exists, for each application, a limiting

consistency above which the passage probability is a function of consistency and other factors. This would provide a direct indication -- and a measure -- of interaction.

Over the range of operating parameters where the concepts are reasonably valid performance data can easily be recorded and applied in various contexts without risk of the sort of interference from composition and reject rate demonstrated here for the Q and T values.

No model of screens or cleaners can ever be demonstrated to be generally valid for all screens and cleaners; validation must be specific to the particular apparatus. It is my hope, however, that the concepts set forth here might provide a framework for the testing and modeling of screens and systems for screening and cleaning.

Literature

1. Nelson, G.: Tappi 64(1981):5, 133. Also in preprint from the 1975 international mechanical pulping conference.
2. Steenberg, B.: Sv. Papperst. 56(1953): ,771
3. Almin, K.-E. and Steenberg, B.: SPT 57(1954):2, 37
4. Kubat, J. and Steenberg, B.: SPT 58(1955):15, 319
5. Steenberg, B. and Kubat, J.: Das Papier 10(1956):5/6, 83
6. Kubat, J.: SPT 59(1956):5, 175
7. Kubat, J.: SPT 59(1956):7, 251
8. Klemm, K.H.: Wochenblatt f. Papierf. __ (1955):7, 261
9. Fredriksson, B.: SPT 87(1984):12, R94

PROJECT REPORT FORM

Project No. 3590
Cooperator Institute exploratory
Report No. 2
Date January 15, 1987
Signed [Signature]

Institute of Paper Science and Technology
Central Files

Measurement of the Double-RefRACTIVE Properties of Paper Webs

An attempt has been made to measure the double-refractive properties, i.e., the light polarizing power of paper sheets. This may have several applications but was done primarily to explore whether such a measurement might be used for rapid assessment of average fiber orientation in paper webs and thin layers of fiber suspensions. The preliminary results indicate that such measurements are feasible when performed on thin tissue, but not on heavy papers or board.

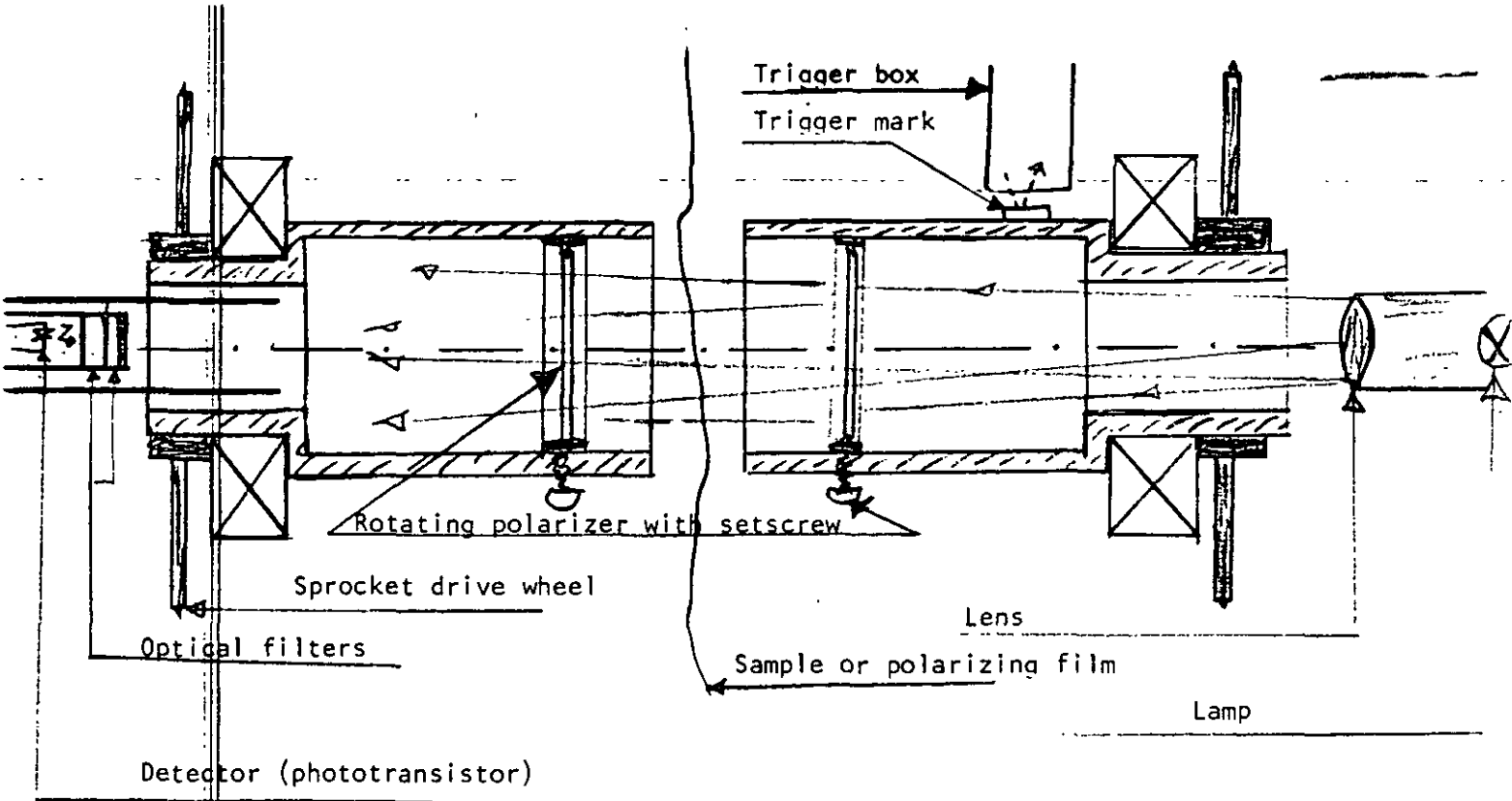


Figure 1. Sketch of experimental arrangement

The experimental setup is sketched in Figure 1. The essential elements are, from right to left, a source of directional incandescent light (a regular microscope lamp), two holders for polarizing filters, each one of which can be rotated by a motor, and a light intensity sensor. In addition, a timing circuit can be used to trigger an oscilloscope trace, as was done in this case, or to evaluate a phase relationship by other means. The polarizing filters can be rotated synchronously or otherwise, and they can be aligned optically by means of a planetary lockable gear. Specifically, in the experiments reported below, the polarizing filters were aligned to give minimum extinction of transmitted light as evidenced by the dc level measured by the photo-sensor.

Adjustments

The device is started and brought up to speed, the light source aligned to maximize the transmitted light intensity and the corresponding dc signal, and to minimize the ac component of the signal. A stationary polarizing film is introduced between the two rotating polarizing filters. This induces a strong ac component in the transmitted light signal. The position of the triggering mechanism is adjusted so that the pulse is aligned with a maximum or minimum of the transmitted light intensity. The setup is now ready for use.

Demonstration experiments

If the stationary polarizing film is rotated through an angle, one can observe on the oscilloscope screen the corresponding change of phase relationship between the triggering circuit pulse and the signal corresponding to transmitted light intensity.

paper webs, specifically rapid determination of average fiber orientation may be feasible. Using a combination of synchronized and asynchronous illumination and detection polarizers, it may be feasible to generate enough information to separate light scattering effects from the directional effects.

These measurements can also be made from a distance using conventional optics. It is also possible in principle to replace the rather awkward mechanically rotating arrangement by modern opto-electronics where the plane of polarization is rotated by other means.

The device described above was demonstrated to Gary Baum on January 14, 1987, and left in his care. Preliminary mechanical drawings were made by Dale Young. One set of copies is filed with the original of this report.

DW/bsb

DATE	REV	REVISION RECORD	AUTH	DR	CK

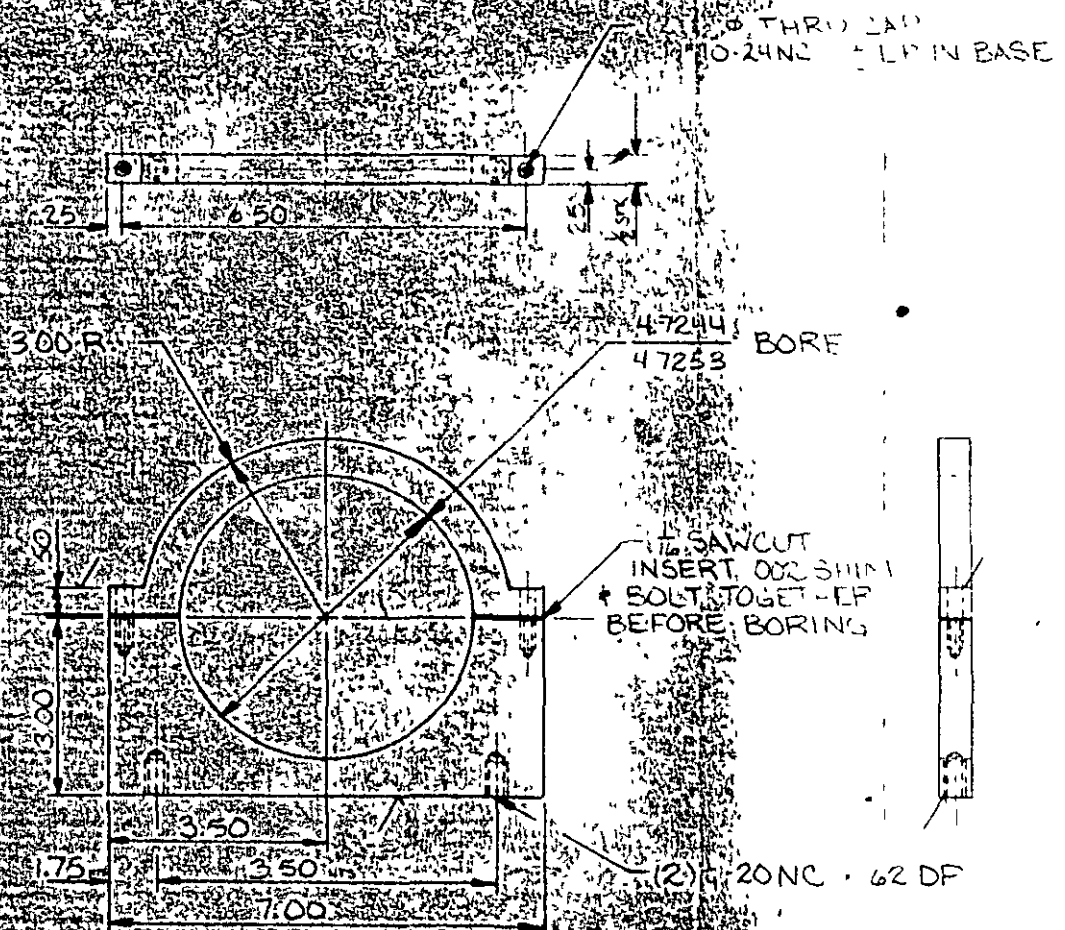


MAT'L: (2) REQ'D 1/2" x 5.00" x .12" PLATE, ALUMINUM

JAN 15 1987

TOLERANCES (UNLESS OTHERWISE SPECIFIED)				THE INSTITUTE OF PAPER CHEMISTRY APPLETON, WI			
DECIMAL	FIBER ORIENTATION		SCALE	DRAWN BY			
± 0.010	DETECTOR		HALF	APPROVED BY			
FRACTIONAL	TITLE						
± 1/16	OUTER BEARING STAND						
ANGULAR	DATE	DRAWING NUMBER		SCALE			
± 0.5	7-9-85	3590-115-3		MADE IN U.S.A.			

DATE	BY	REVISION RECORD	AUTH	DR	CK



(2) REQUIRED
 MAT'L 612-700 PLATE ALUMINUM

TOLERANCES (UNLESS OTHERWISE NOTED)				THE INSTITUTE OF PAPER CHEMISTRY APPLETON, WI.			
DECIMAL	FIBER ORIENTATION DETECTOR		SCALE HALF	DRAWN BY <i>[Signature]</i>		APPROVED BY <i>[Signature]</i>	
FRACTIONAL	TITLE INNER BEARING STAND						
ANGULAR	DATE 7-9-86	DRAWING NUMBER 3590-1-13-84					

ALL DIMENSIONS IN INCHES UNLESS OTHERWISE NOTED
 MADE IN U.S.A.

PROJECT REPORT FORM

*... removed
having circulation) see*

✓ Project No. 3590
Cooperator Institute
Report No. 1
Date August 30, 1985
Signed *DW*
Douglas Wahren

Institute of Paper Science and Technology
Central Files

MEASUREMENT OF MOTTLE - AN EXPLORATORY STUDY

SUMMARY

A small project was initiated by an inquiry from a member company. It explored some possibilities for instrumental evaluation of mottle of paper and board over a wide range of colors and luminance factors. It is concluded that a simple, straightforward instrumental method could be developed which would grade similar samples adequately on the basis of mottle intensity. Some further research, involving panel evaluations of mottle, would be required in order to develop a method which would evaluate mottle adequately for process control purposes and which would yield a consistent measure of mottle which would be independent of the color and luminance factor of the sample over a broad range.

INTRODUCTION

Thirteen samples of board, produced by a member company, were received on August 19, 1985, and the possibilities of developing an objective instrumental method for evaluation of the visual perception of mottle have been assessed. Efforts have met with some degree of success in that it is indeed possible to obtain good, clean, reproducible signals from all the samples of board. The signals do correspond quite well to simple evaluations of mottle made by myself and a few associates when restricted to a limited range of color. For instance, there is no problem of grading all the blue samples (1-3) or the beige samples (11-13), etc. The problem of how to generate a signal which would correspond to subjective judgment independent of color has not been resolved. This is not due to technical difficulties but to the degree of effort which must be put into the subjective evaluation part. Comparing, for instance, a blue sample to a gray one, or to one dyed deep magenta, is like comparing apples and oranges and one must be careful in making such comparisons correctly or else limit the method to a reasonably narrow range of colors and luminance factors. For practical purposes, however, this should not be a big problem.

For this preliminary study, I used available equipment not necessarily ideally suited for routine use in a production environment. It would take considerable effort to develop a rugged instrument which could be used for routine quality control. It might be fairly easy, however, to develop an instrument which could be used for occasional on-line measurements and where the sensor would be hand-held. This would get around the problem of manufacturing or purchasing the most expensive part, i.e., the mechanical scanning device.

EXPERIMENTAL APPROACH

There is no generally accepted definition of mottle but instrumental assessment of the visual perception of unevenness is discussed in the literature on photographic materials, print quality, and quality of formation in paper and board. Appendix 1* discusses some of the concepts. The basic idea in this exploratory phase is to explore a system which measures the variation of reflectance from a paper surface in such a way as to emulate the sensitivity of the eye and some basic processes involved in human visual perception of stochastic images.

Color:

The typical sensitivity of human vision is centered around 550nm, i.e., in a yellow-green part of the spectrum. Some experimentation led to the adoption of a combination of a simple low voltage incandescent bulb, a phototransistor ECG 3038, 2mm of Corning 3-77 glass filter and 1mm Hoya CM 500 glass filter. This combination produced a very linear relationship between the measured signal and the luminous reflectance as measured by standard ISO methods (Y-filter).

Intensity:

It is well-known (Weber-Fechner's law) that human vision, like many other senses, has a logarithmic characteristic. Hence, it is desirable to employ a circuit with a logarithmic sensitivity. As it turns out, however, the variation of interest is very small; the coefficient of variation of reflectance ranging from

* B. Norman and D. Wahren, "The influence of paper formation on the evenness of solid prints", proceedings of 14th EUCEPA Conference, Budapest, October 1971.

about 1/2% for a good sheet to 3% for a mottled sheet. Within such a narrow range, even a perfectly logarithmic relationship can be closely approximated by a straight line. Still, a logarithmic circuit was employed because it also offers other advantages, as will be explained below.

Resolution:

The average person with good vision can resolve detail down to about 0.1mm when using foveal vision. Mottle, however, although not well defined, in my mind is associated with rather larger scale variations, for instance 1/16" to 1". Two resolutions were explored in this investigation, namely a circular area with a diameter of 2mm and a circular area of the same size but with many optical fibers in contact with the sample picking up extra detail.

Signal Processing:

As shown in the appendix, it is desirable in theory to measure the RMS value of the derivative of the logarithm of the reflected light intensity. For the first several series of measurements a full-fledged RMS meter was employed in parallel with a precision AC average measuring circuit. The degree of correlation was very high and, since the AC averaging circuit can be engineered easily to averaging over suitable periods of time, that is the one which was used for the data which are reported.

A couple of series of measurements were made on signals employing electronic differentiation of the logarithmic signal. As pointed out in the appendix, this measurement should correlate strongly with a measurement of the undifferentiated signal provided other conditions of the measurement are kept constant. This was

found to be the case and, since the differentiating circuit inevitably produces extra noise, all reported measurements were made using:

The average of the AC component of the logarithm of the reflected light intensity.

A range of conditions for scanning the sheet and bandpass-filtering the signal was explored. The final bandpass filter had lower and upper time constants of 0.4 and 0.001 seconds respectively, employing simple RC-circuits.

Scanning Pattern:

When employing a circular scanning mode, several scanning patterns were investigated, namely circular, elliptical and sinusoidal. Various constant scanning speeds, of up to 15" per second, were employed. In order to get a representative sample, however, it was necessary to move the scanning pattern manually across the sheet which did not help reproducibility. A complex elliptical scanning pattern was employed quite successfully. It is shown in Figure 1. It is obvious, however, that the scanning pattern did not sample the surface uniformly.

The most effective scanning pattern, and the one which was subsequently used for all the data reported, is a simple sinusoidal pattern, shown in Figure 2.

Obviously the scanning velocity varied from zero at the turning points to a maximum. The scanning frequency employed was 0.62 complete cycles per second, giving a maximum scanning velocity of 12.6"/s or 320mm/s. Because of the filtering arrangement mentioned above, most of the signal was derived from the central position of the sheet. This mode of scanning provides a good running

average of the nonuniformities encountered and it is easy to avoid smudges, printed text, etc. The scanning pattern can easily be reversed such that MD and CD information can be obtained separately. The data reported below refer to scanning patterns located as shown in Figure 2. Some differences were observed when scanning in the machine and cross-machine directions. Sample No. 2 in particular, which was badly mottled, showed quite large differences between MD and CD.

HARDWARE PRINCIPLES

Many different principles could be employed for sensing reflectance variations from paper sheets. The obvious way today would be to use a high resolution TV camera and an image analyzer, digitizing the picture and analyzing it by computer. This may be a real possibility for the future but, considering the extremely narrow range of contrast, it is probably a difficult route to take.

Paper samples could be mounted on spinning disks or cylinders and the sensing head could be traversed and/or oscillated radially or axially respectively. Illumination would have to be provided in the scanning head in order to obtain uniform conditions over the entire scan surface. These possibilities certainly might be viable for a laboratory or routine production control instrument. The reflectance signal is highly sensitive to the distance between the paper and the light source as well as the measuring aperture, hence, good precision and mechanical stability are required. Employing a spinning disk would make it difficult to separate measurements in the machine and cross-machine directions. Employing a rotating cylinder would necessitate, as a minimum, a track-and-hold circuit to carry the signal processing across sheet discontinuities caused by taping or

otherwise holding the sheet down.

If large samples are employed it would be possible to use a stationary sensing system and moving paper sample past the scanning head. Such a system, but a very slow one, is sold under the trade name Thunderscan. It relies on an Apple Computer, Inc. Imagewriter printer to move the paper and a Macintosh computer to record the data. A simplified system could be used for on-line measurements. It might be possible to develop a mechanically simple, hand-held sensing head to be used on the reel.

System used:

For the present exploratory phase, an X-Y recorder with an electrostatic paper hold-down was used. The pen was replaced with a fiber light guide. The X and Y axes were fed suitable signals to provide the scanning patterns shown above.

The principles of the optical/electronic system are shown in Figure 3. An incandescent lamp shines light in through one of the branches of a Y-shaped light guide. The light illuminates the sample through the common leg of the light guide, which is fastened to the pen holder of the X-Y recorder. The other leg of the light guide receives the reflected light and carries it back to a phototransistor. The fibers from both light guides are well mixed at the sensing point which is fastened to the pen holder of the X-Y recorder.

The reflected light passes through optical filters before reaching the phototransistor. The filters can be rather easily exchanged. The phototransistor is directly connected to a 15 volt regulated power supply and to a logarithmic amplifier, the input terminal of which is held at ground potential. Hence, the

portions of both wires connected to the phototransistor are always at constant potential; the device is essentially current-connected so that cable capacitance has very little influence on the frequency response. Extremely low currents are employed, but careful double shielding and single point grounding lowered 60 and 120 cycle hum to undetectable levels. The frequency response as tested against the sweep of an oscilloscope is good at least up to 50,000 kHz.

THE FIBER-OPTIC SENSOR ARRANGEMENT

The distance between the fiber optic cable and the sample, denoted by "X" in Figure 3, influences the reflectance signal dramatically. The reflectance signal has a maximum at about $X = 2\text{mm}$ and drops about 40% when $X = 0$, i.e., when the fiber light guide cable is allowed to rest on the sample. The reason for this is that light emerging from the illuminating fibers emerges as cones and, similarly, light is collected by the measuring fibers from a cone-shaped volume. When the optical fibers are in contact with the paper, light has to travel down into the sample and be reflected back to the sensing fibers by internal reflections in the sheet. If the fiber light guide cable were "ideally" made, no light would be transmitted from the illuminating to the sensing fibers if the end of the light guide were put in contact with a black substrate.

When the distance X is slightly increased, the sample surface is illuminated and the sensing fibers can pick up the reflected light more efficiently. At large distances, X, between the light guide cable and the sample, illumination and sensing will deteriorate rapidly. Because neither illumination nor sensing are made diffusely, the usual square of the distance law does not necessarily apply.

It should be obvious from the above discussion that it is necessary to keep a

very well defined distance between the sample and the light guide. Two conditions were used in this study; one when $X = 0$ and one when $X = 2.5\text{mm}$. In the latter case, the light guide was enclosed by a black piece of medium-soft plastic, tapered down to a circular opening having a diameter of about 2mm.

CALIBRATION AND INITIAL RESULTS

Figure 4 shows the luminance factor (R_0 using the Y-filter) plotted against the DC level out of the logarithmic amplifier. The uppermost line denotes the case when the fiber light guide was held at 2.5mm distance from the sheet and a 2mm diameter area was measured. The lower line shows data obtained with the fiber light guide in direct contact with the sample. Reflectance values for all board samples have been plotted.

It is apparent that, in both cases, the optical-electronic arrangement used yields the expected linear relationships between output voltage and the logarithm of the luminance factor of the sample. Incidentally, the output voltage was evaluated as the average of a scan covering almost the entire surface of each sheet, whereas the luminance factor was the average of 8-10 measured points using a standard reflectance instrument.

The regression equations are listed in the diagram. The important number corresponding to the sensitivity of the measurement is the coefficient for the logarithmic term. The electronic circuit is expected on theoretical grounds to give a value of 59 mV/decade of reflectance. The actual value when the 2.5mm distance was used was 55.3. The deviation from 59 can be explained on the basis of internal reflections inside the tapering plastic sensor tip which was, of course, not perfectly black.

With the probe in direct contact with the sample, a higher coefficient, 75.2 mV/decade was obtained. This can be qualitatively understood as being a function of the strange internal reflectance process employed and mentioned above. This aspect has not been properly investigated.

Since both relationships are accurately linear, the coefficients for the logarithmic terms can be used for calibration purposes. The constants (624 and 611 respectively) are of no consequence in what follows and can be adjusted at will.

Electronic Calibration:

The circuits employed operational amplifiers and high precision resistors; remnants from an old analog computer. Hence, amplification factors are accurately known. Consider an electrical signal e as the output from a logarithmic amplifier:

$$e = -a + b \log R$$

where R is the reflectance of the sample. For small signals, this relationship can be differentiated to yield

$$de = \frac{b}{\ln 10} \cdot \frac{dR}{R}$$

For a randomly varying signal then, the coefficient of variation of reflectance becomes

$$V(R) = \frac{\ln 10}{b} \cdot \sigma(e)$$

where $\sigma(e)$ denotes the standard deviation, or RMS (Root Mean Square) value of the electrical signal. The parameter b is the one discussed above which, in this case, has the value 55.3 or 70 mV/decade.

In combination with the amplification factors employed, the resulting calibration when the probe was in contact with the paper was 0.674% variation of reflectance per 100 μ amperes, 0.674%/100 μ A. With the probe at a distance of 2.5mm from the sample, the sensitivity was 0.427%/100 μ A.

These calibrations held up to within the repeatability of readings (perhaps 2-3%) over a period of 10 days and were not influenced by amplifier drift, etc.

RESULTS

Table 1 lists notes on the "look-through" of the board samples used. Table 2 lists their luminance factors and brightness. Figure 5 shows the spectral distribution of reflectance of four representative board samples. Table 3 summarizes selected results of measurements of mottle.

The Two Optical Arrangements:

Diagram 6 shows the mottle signal obtained with the probe in direct contact with the sample plotted against the mottle signal when the probe was at a 2.5mm distance from the sample. The straight line denotes where the points would be plotted if the two methods of measurement were actually measuring the same thing. This line has been calculated to take into account the two different b values, differences in amplification, etc. On the inside of the two scales, the magnitude of the coefficient of variation of reflected light, taking the same factors into account is noted.

It is obvious from the diagram that, when the probe is in direct contact with the sample, more information is picked up. Inspection of the signal on the oscilloscope indicated that higher frequency components are present. This is to be expected when the fiber light guides are in direct contact with the sample. The two sensing methods are correlated in a general way, but differences in sheet structure certainly can be expected to "ruin" the correlation.

The lower resolution method, i.e., with a probe 2.5mm from the sample and employing a measurement area of 2mm in diameter, is probably the more relevant one because it is less influenced by fine detail in or on the sheet surface. This appears to be more consistent with the concept of mottle than if fine embossing patterns or individual dyed fibers were to influence the result.

Note that this diagram illustrates the statement made before that the mottle intensity is of the order of .5-1.5% using the lower resolution and up to 3% using the higher resolution method.

Figure 7 illustrates that the mottle, when expressed as the coefficient of variation of reflectance, appears to decrease with increasing luminance factor of the sample (still, sample No. 2 deviates from the "norm").

The same data are replotted in Figure 8 as the coefficient of variation of reflectance times the logarithm of the luminance factor (times an arbitrary constant). This method of display makes samples 2 and 10 stand out as particularly mottled ones.

DISCUSSION OF RESULTS

Note, in Figure 6, that the three magenta samples, 4, 5 and 6, are the worst ones when evaluated by either method and that the badly mottled sample, No. 2, gets a better reading. This points out two major problems in the design of an appropriate instrumental method for evaluation of mottle.

1. Subjective perception of mottle depends on the luminance factor of the sample.
2. The coefficient of variation of reflectance, which is relatively easy to measure, depends not only on the bulk reflectance in the conventional (Kubelka-Munk) sense, but also on surface reflectance. For very dark sheets, surface reflectance may dominate the reflectance pattern.

Surface reflection depends on the surface smoothness, which in turn is a function of calendering or embossing, and the formation of the sheet. Bulk reflection depends on nonuniformity of dye distribution, fiber orientation and sheet density, all of which may depend on various processing factors.

In the very simple survey made, everybody judged samples 1 and 3 (light blue) to be less mottled than samples 7, 8 and 9 (light gray). The measurements indicated that the blue samples had a larger coefficient of variation of reflectance than the gray ones. This might have been interpreted to mean that people tend to judge blue as being cleaner than light gray, i.e., it might put use of the luminance concept (Y-function) in doubt. It was indeed possible to reverse the order of instrumental classification of the samples by shifting filters into the blue (brightness) region of the spectrum. Such a shift, however, caused new discrepancies in the ranking of other colored samples.

I believe that it is inappropriate to use anything but a major emphasis on the yellow/green part of the spectrum where the human visual senses are centered. The reason for the discrepancy is probably due to a decline in perceived mottle with decreasing luminous reflectance combined with an increased relative importance of surface reflections at lower reflectance. For extremely dark sheets, an instrument senses surface reflections superimposed on black. This gives a strong signal. For a perfectly reflecting sheet, almost by definition, there is little variation of reflectance. These questions of sensing and perception need to be analyzed as well as the purely physical questions of the importance of surface reflections for dark sheets.

A good method for instrumental determination of mottle, to be used for process control purposes, should preferably yield the same result for two (theoretical) paper or board samples differing only in the magnitude of the light absorption coefficient of the dye (same formation, calendering, etc.). I believe that a reasonably good approximation to this ideal case can be developed on the basis of further theoretical analysis. As a first crude approximation, and without much theoretical backing, $V(R) \cdot \log R_0$ in diagram 8 was tabulated and plotted. Plotting data, Figure 8, singles out samples 2 and 10 as the bad ones, but does not give sufficient emphasis to the deep magenta-colored samples. This kind of simple data transformation could easily be implemented by simple electronics. I have such data tabulated as "AC ave. $\cdot (e_1 - 611)$ ".

CONCLUSIONS

At this point I believe we have a simple method which will grade similar samples quite adequately. Please inspect the measured data and compare to your own perception of mottle in the samples. Unfortunately, several of the samples have been smudged and even marked by the several different sensing heads used. It would be necessary to produce a new set of samples, preferably multiple samples for each grade, before any further meaningful work could be done.

In order to test any method to be developed, it is necessary to have available a fairly wide range of samples, such as the ones used in this investigation, where all the samples have been graded for mottle by a panel of suitable judges.

Development of new, reliable and millworthy instrumentation is always a costly undertaking. I believe that the essential principles of mottle measurement are sufficiently understood to allow development of a meaningful method of measurement. This could be done slowly and gradually up to a lab prototype by interesting a student to take on the task. The time of completion would be on the order of 1½ years. Cost to the cooperator would be very small or nonexistent but we would still have to find the necessary funds at the end of the project to build a millworthy prototype.

Another approach which would be much quicker would entail a cooperative effort where we discuss and decide on the type of scanner to be used (including, possibly, an on-line fixed or hand-held version) and where the cooperator would become actively involved in supporting the development and testing of prototypes.

TABLE 1

NOTES ON LOOKTHROUGH

No. 1:

Well formed sheet. Some light spots due to small droplets or pick outs.

No. 2:

Small scale, grainy formation. Bad suction roll marking. Some pick outs.

No. 3:

Very well formed sheet. Very few light spots and only a couple small, heavy spots.

Nos. 4, 5, 6:

Of the three magenta samples, Nos. 4 and 5 are very similar; fairly well closed with large smeared out flocs, ranging in size from small to several inches, whereas No. 6, although generally similar, appears to have worse formation on a very large scale, i.e., several inches.

No. 7:

Well closed transverse flocs. No evidence of crushing.

No. 8

Well closed sheet with some streaks.

No. 9:

Small scale, grainy, crushed, with some large flocs and pick outs.

No. 10:

Medium sized, intense flocs separated by very thin areas. Looks like jet overspeed relative to wire.

Nos. 11 and 12:

Small scale, very grainy formation. No. 11 is grainier than 12. The sheets look crushed or else having pick outs.

No. 13:

Well closed but with large flocs. No evidence of crushing.

TABLE 2

Sample No.	Luminous reflectance %	Brightness, %
1 Lt. blue	47.9	60.1
2 Lt. blue	46.6	58.9
3 Lt. blue	48.0	60.4
4 Magenta	10.0	7.78
5 Magenta	9.1	6.76
6 Magenta	9.5	7.02
7 Gray	62.8	57.3
8 Gray	62.8	57.2
9 Gray	58.8	52.6
10 linerboard brown	30.2	20.5
11 Beige	52.7	36.2
12 Beige	52.7	36.3
13 Beige	53.9	37.4

TABLE 3

Sample No.	Sensor in contact with sample						Sensor 2.5mm off Sample			
	e_1		AC ave. μA		AC ave. $\cdot \text{Log } R_0$		AC ave. $\cdot (e_1 - 611)$		Front	
	Front	Back	Front	Back	Front	Back	Front	Back	DC mV	AC μA
1 Lt. blue	734	735	250	200	420	336	30.8	24.8	715	140
2 Lt. blue	735	735	330	350	551	584	40.9	43.4	716	230
3 Lt. blue	735	735	200	200	336	336	24.8	24.8	715	130
4 Magenta	685	685	350±	380	350	380	25.9	28.1	677	340
5 Magenta	684	685	400	400	384	384	29.2	29.6	679	300
6 Magenta	685	686	410	380	401	372	30.3	28.5	678	300±
7 Gray	747	748	150	155	270	279	20.4	21.2	724	125
8 Gray	747	748	160	135	288	243	21.8	18.5	723.5	105
9 Gray	745	746	210	170	372	301	28.1	23.0	722.5	140
10 linerboard brown	723	723	350	350	518	518	39.2	39.2	706.5	225
11 Beige	741	742	210	175	362	301	27.3	22.9	720	130
12 Beige	741	742	210	185	362	319	27.3	24.2	719	135
13 Beige	743	743	195	150	338	260	25.7	19.8	720	135

Ranking FRONT sides:

AC ave. 7,8,13,3,9/11/12, 1,2,4/10,5,6
 ACave. $\cdot R_0$ 4,5,6,7,3,8,13,10,11/12,1,9,2
 ACave. $\cdot \text{Log } R_0$ 7,8,3,13,4,11/12,9,5,6,1,10,2

Ranking BACK sides:

8,13,7,9,11,12,1/3,2,10,4/6,5
 8,13,7,9/11,12,1/3,6,5,4,10,2

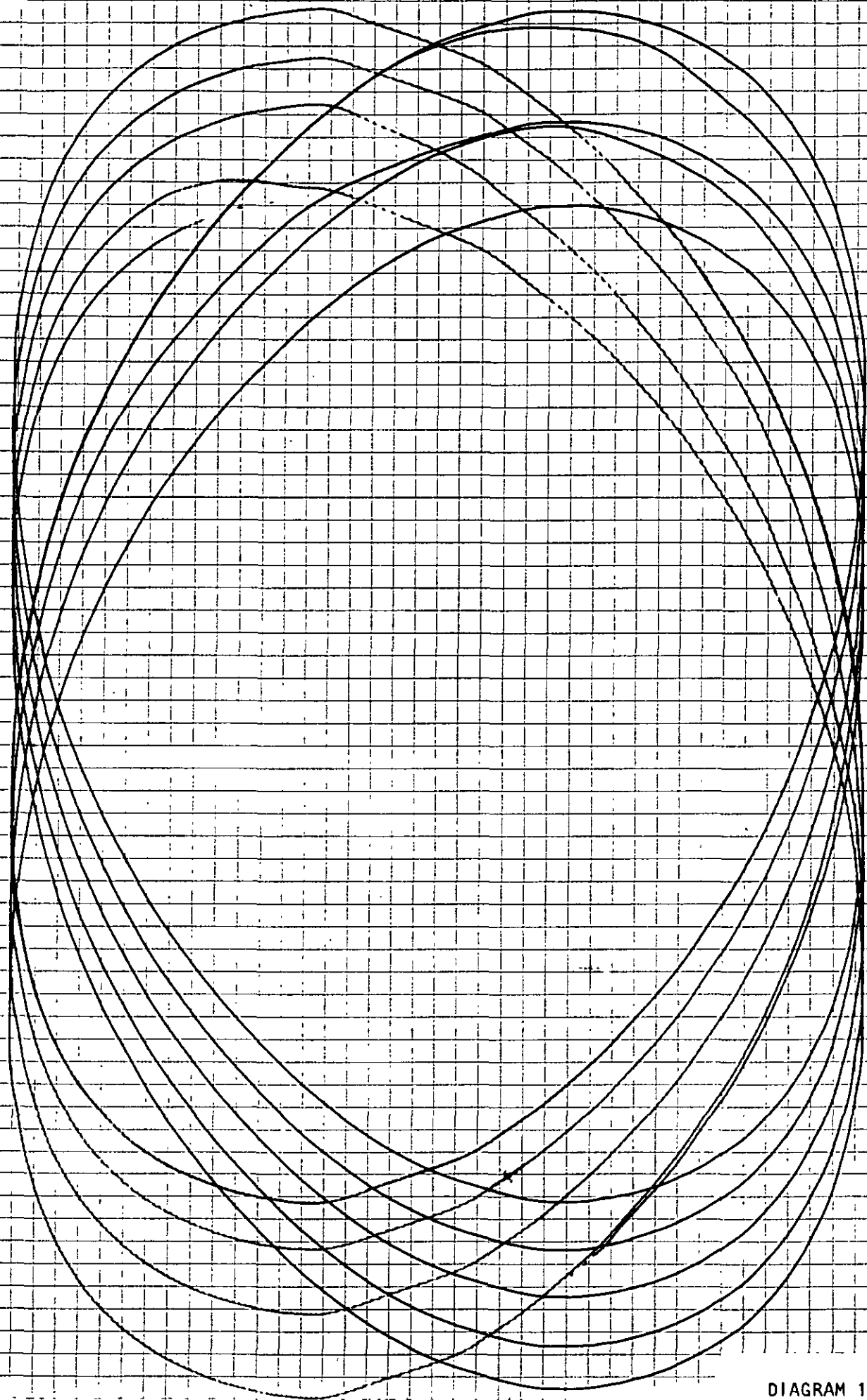


DIAGRAM 1

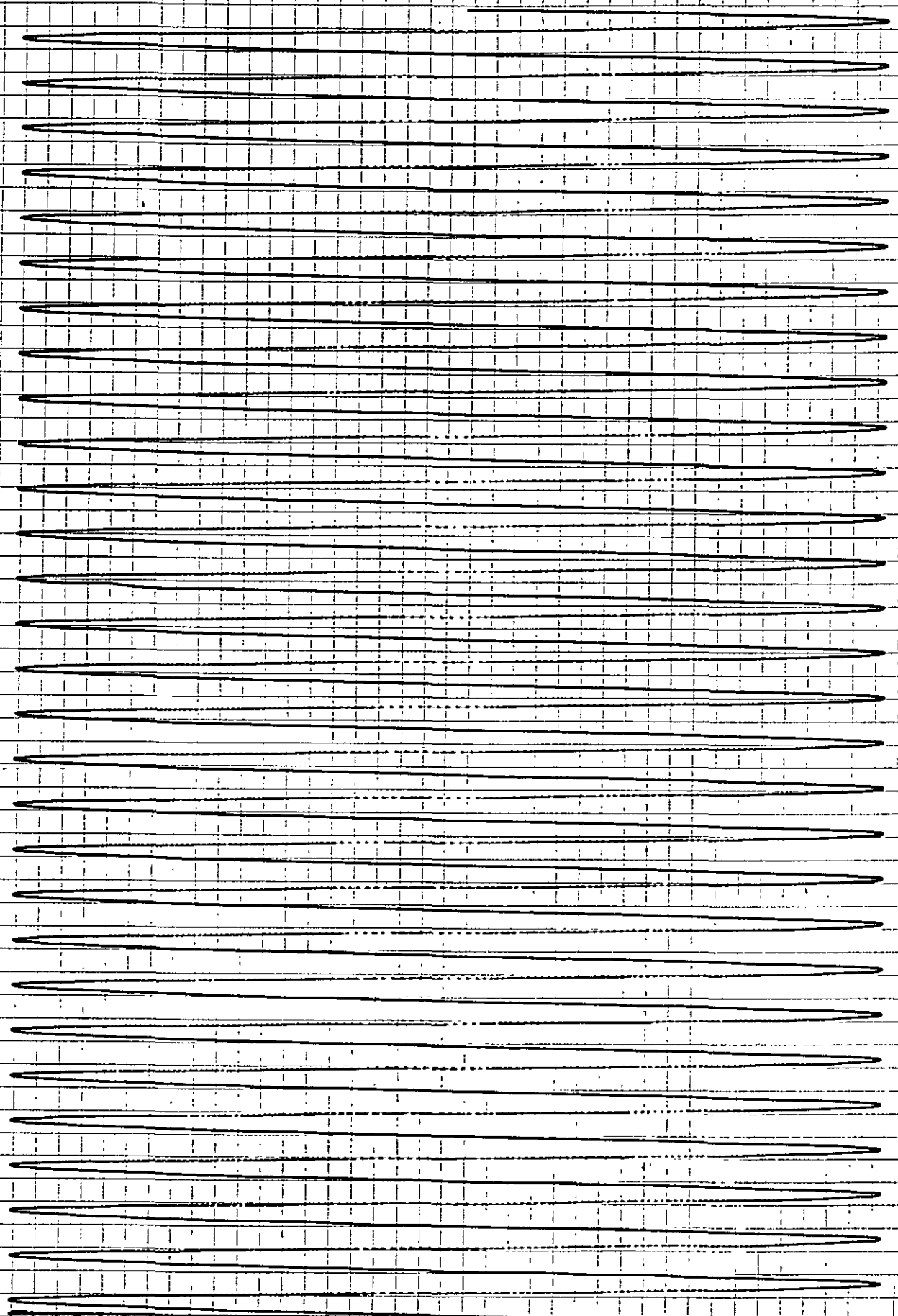


DIAGRAM 2

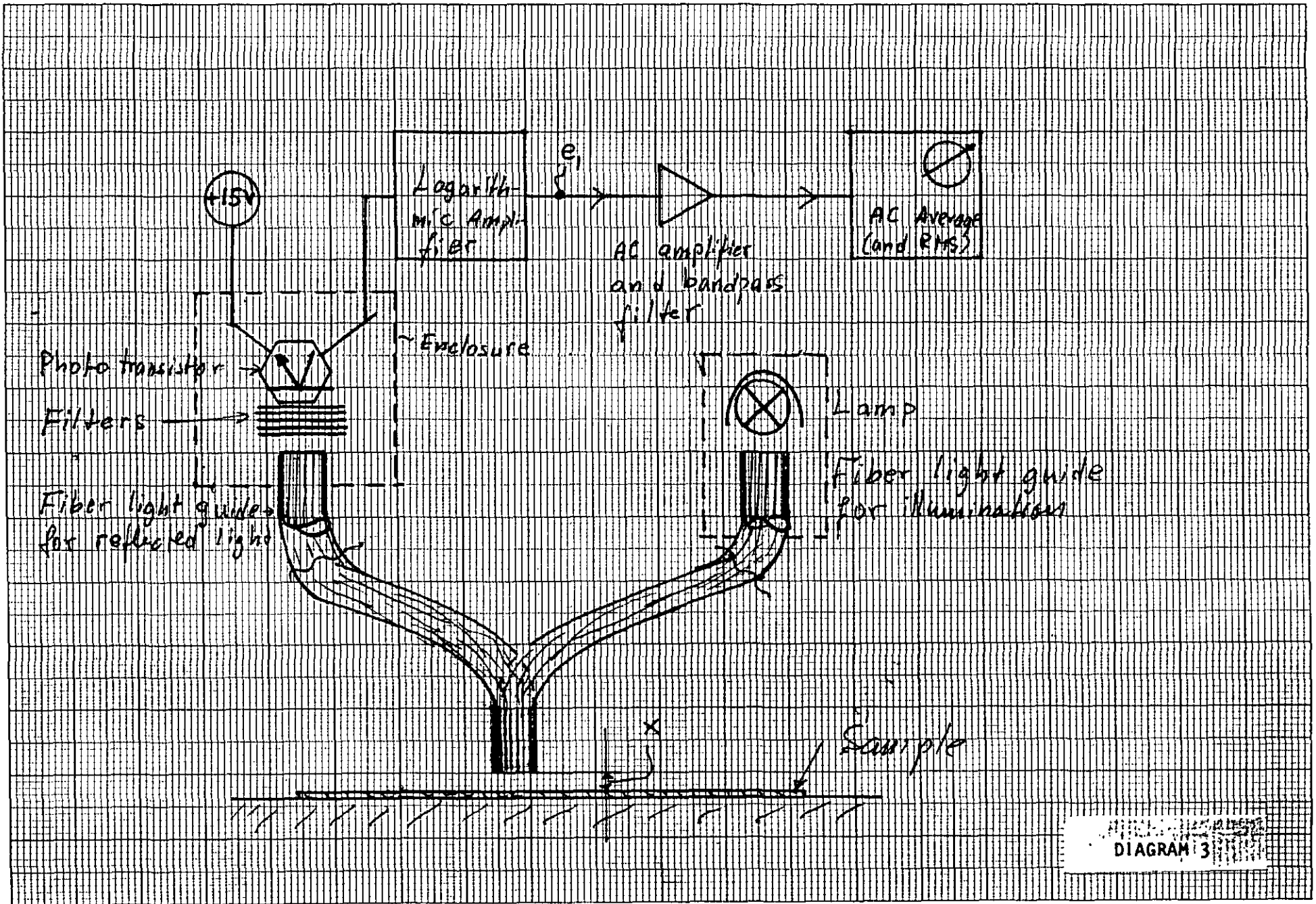
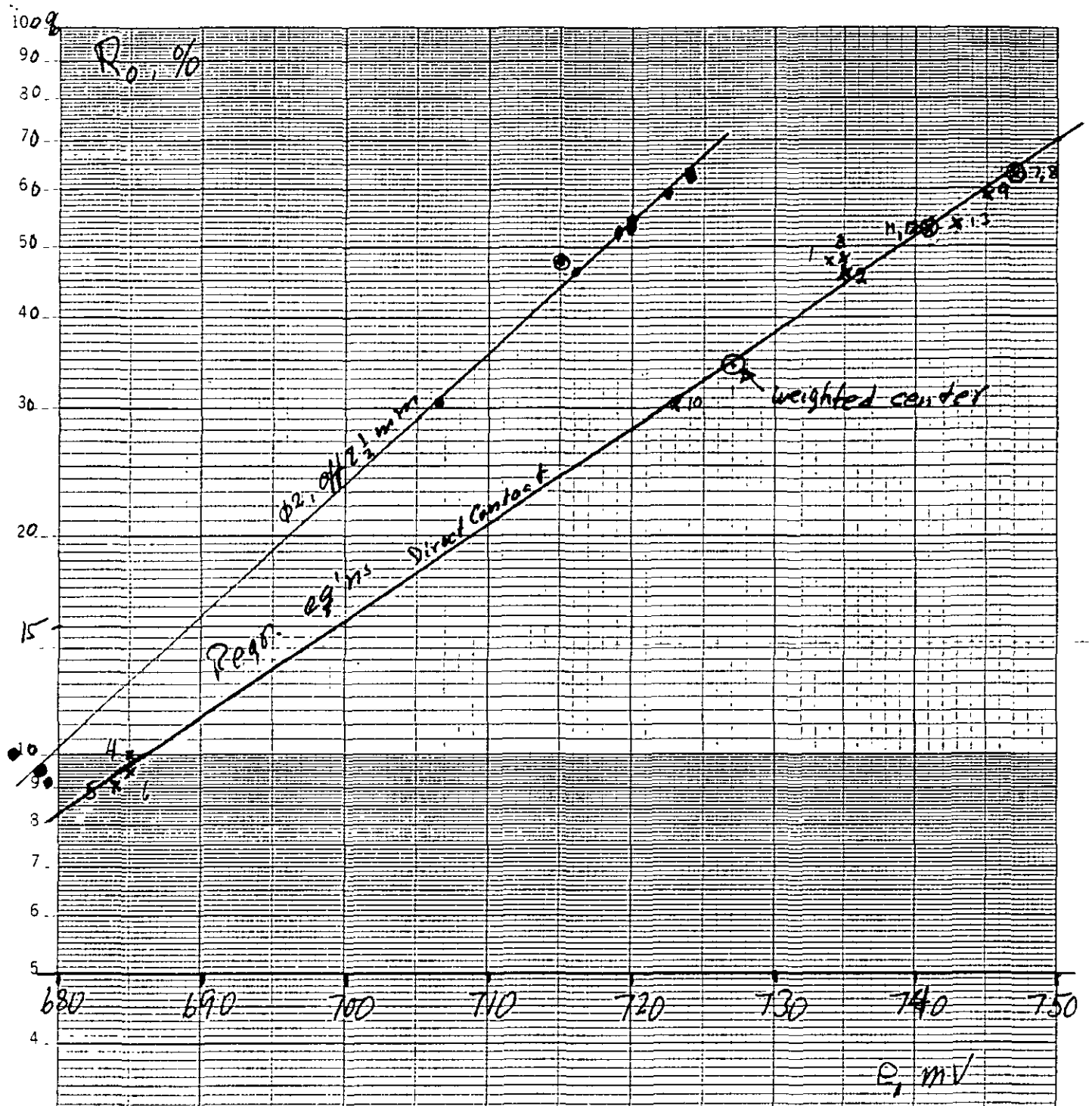


DIAGRAM 3

46 4970

K·E SEMI-LOGARITHMIC #2 CYCLES X 70 DIVISIONS
KEUFFEL & ESSER CO. MADE IN U.S.A.



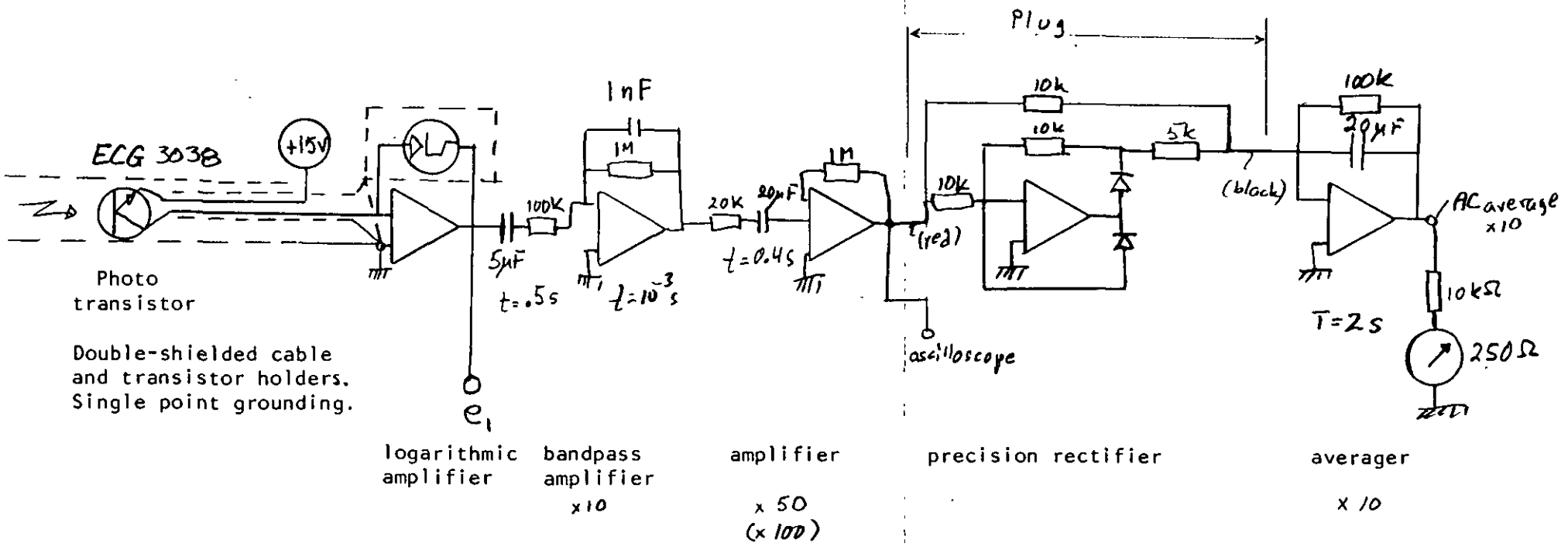
Dir. Contact: $e_1 = 611 + 75.2 \cdot 10 \log(R_o)$

Corr. coeff = 0.998

$\phi 2, \text{off } 2 \frac{1}{2} = e_1 = 624 + 55.3 \cdot 10 \log(R_o)$

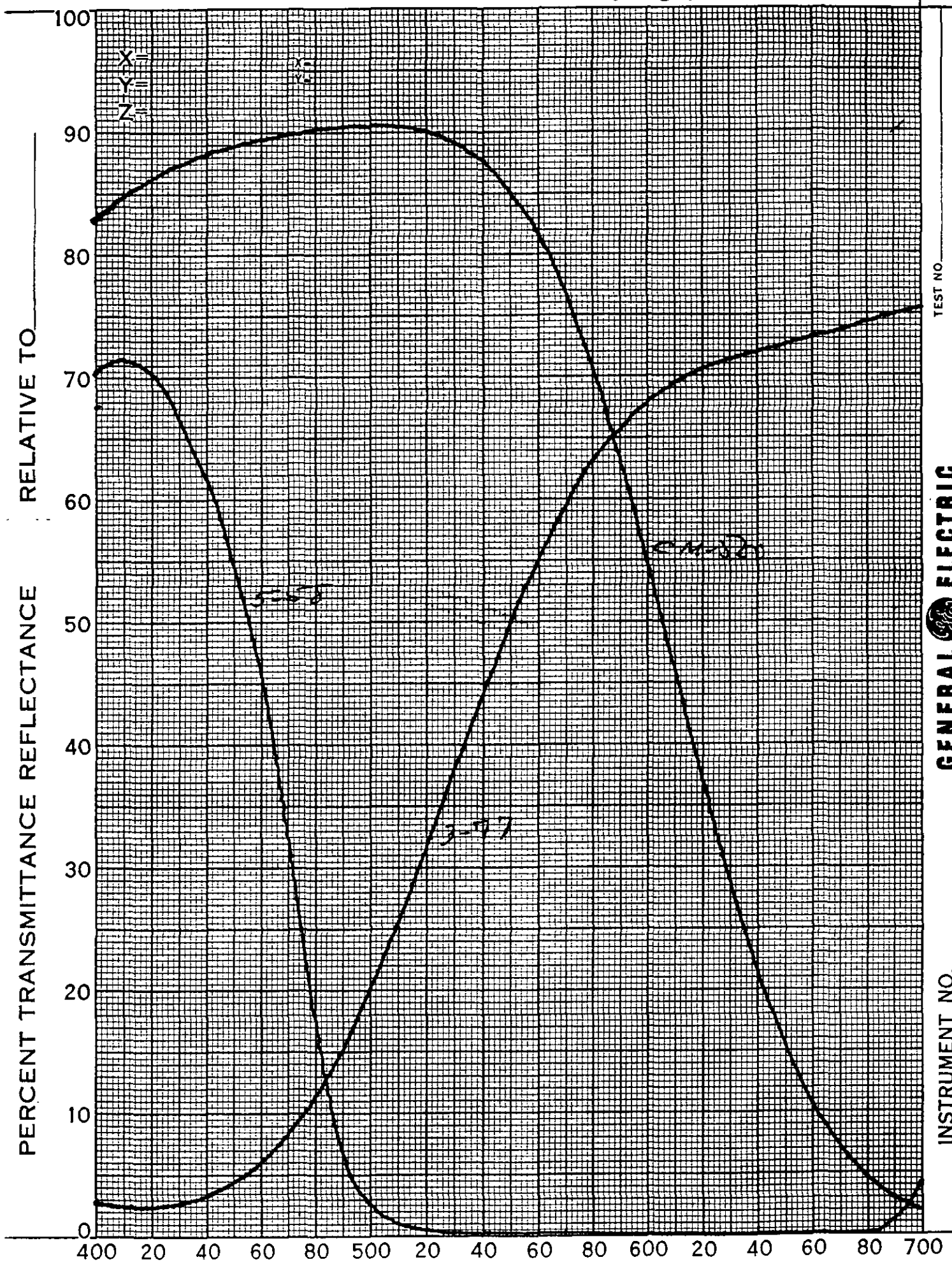
Corr. coeff = 0.998

DIAGRAM 4



for internal report only
 8/27/85

Filter transmission curves, For internal use only.

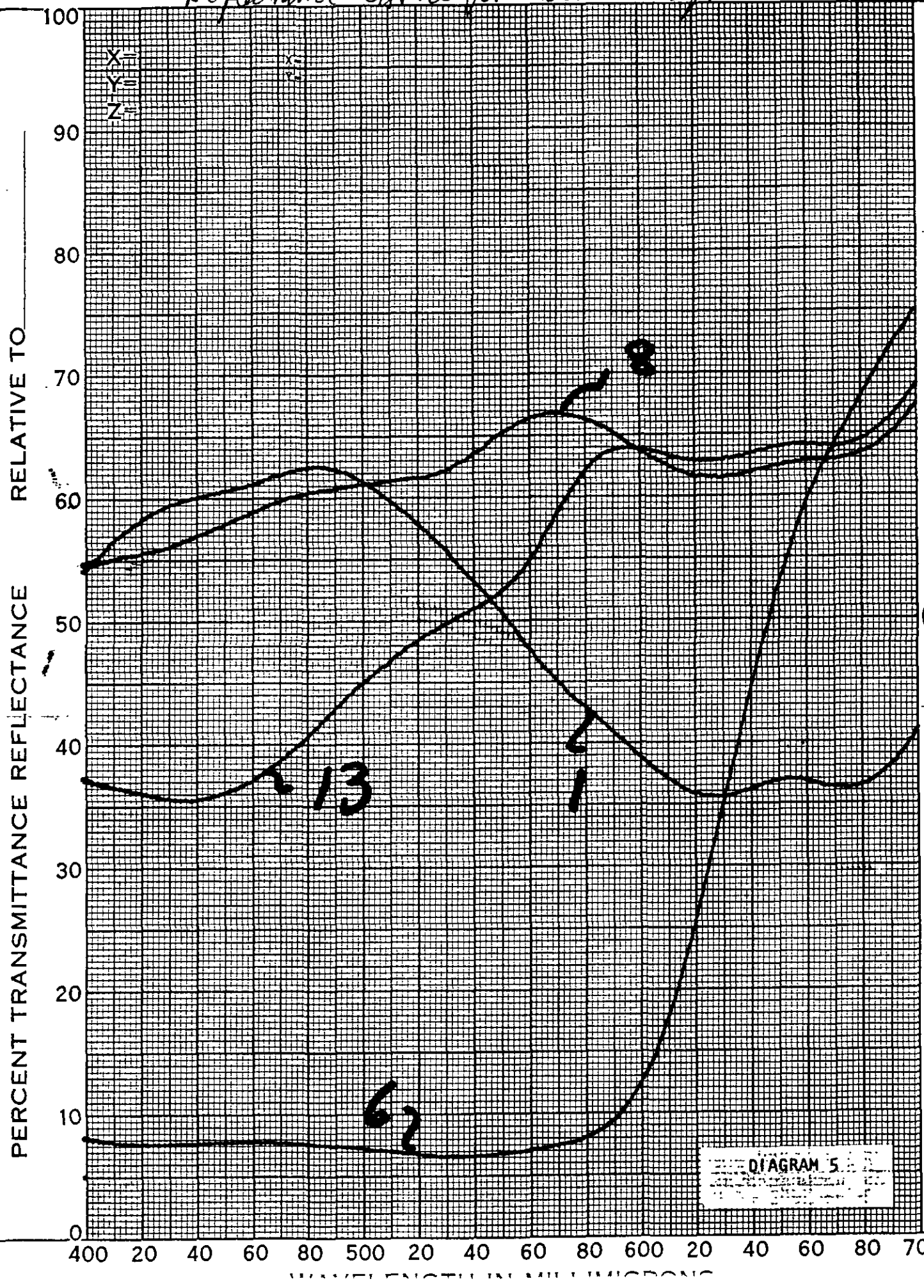


TEST NO.
BY

GENERAL ELECTRIC
RECORDING SPECTROPHOTOMETER

INSTRUMENT NO.

Reflectance curves for some samples

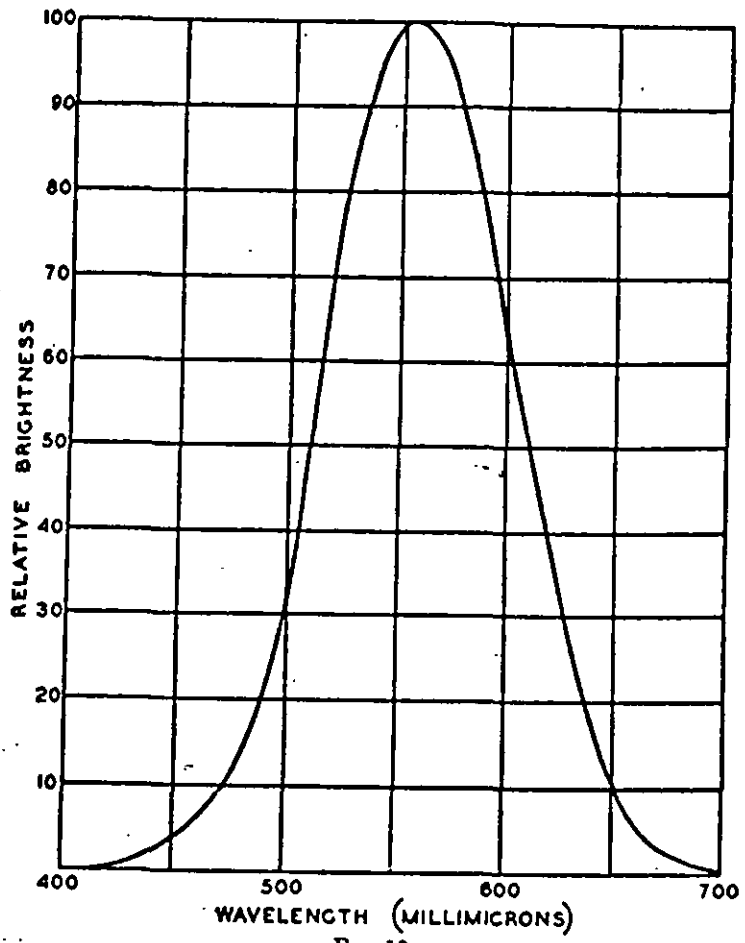


TEST NO. _____
BY _____
DATE _____

GENERAL ELECTRIC
RECORDING SPECTROPHOTOMETER

INSTRUMENT NO. _____

DIAGRAM 5



CIE II. C*Y Function

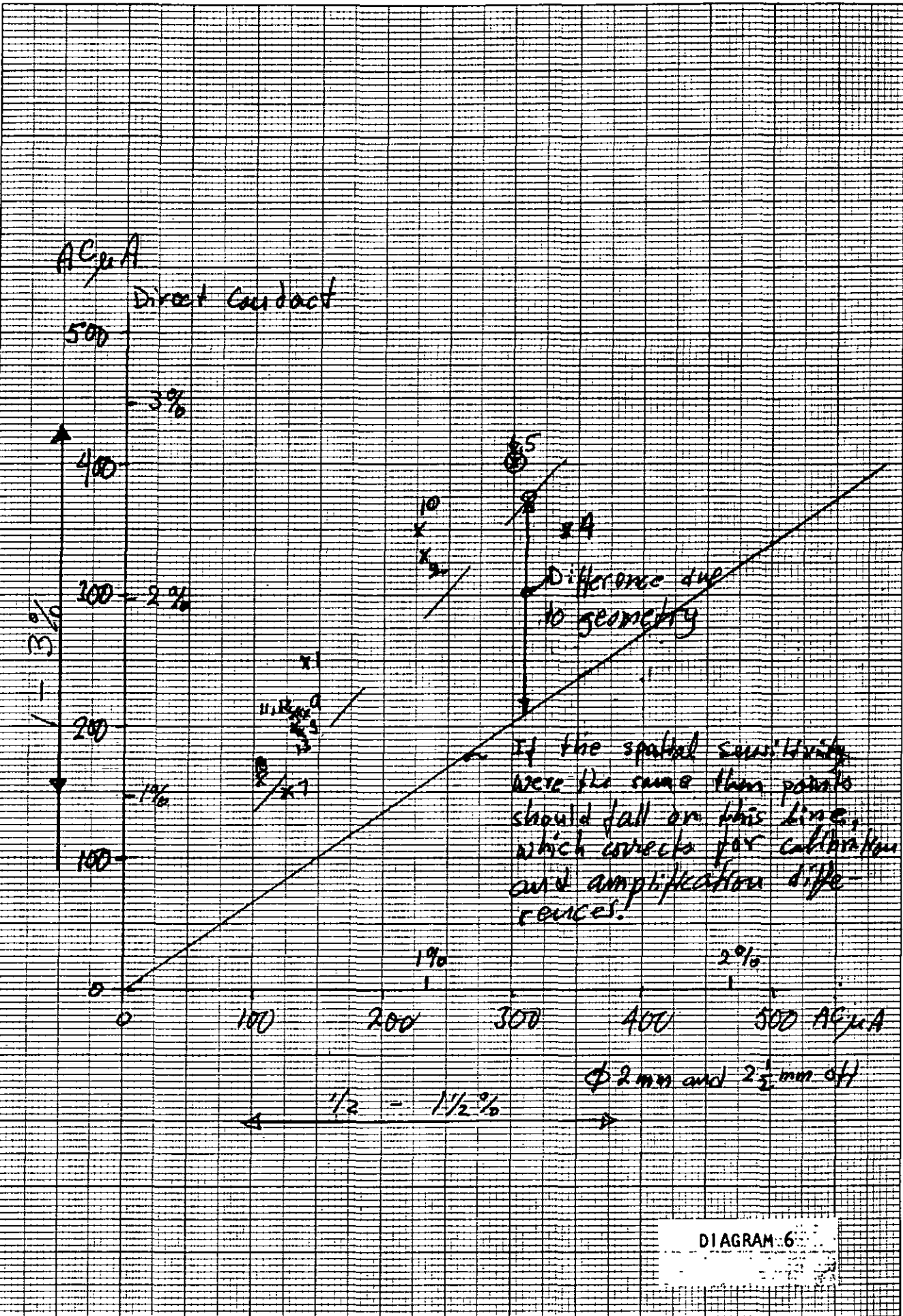


DIAGRAM 6

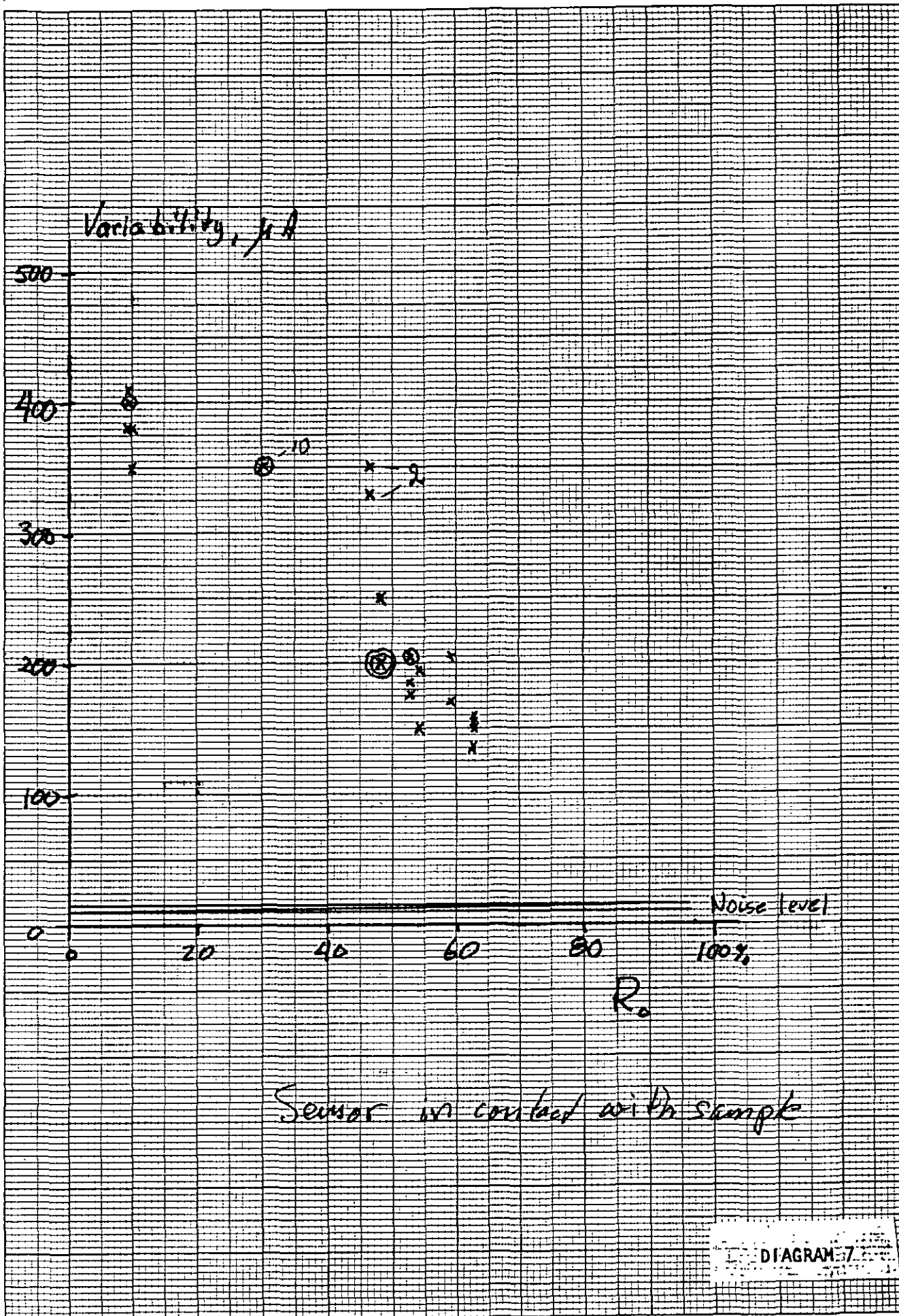


DIAGRAM 7

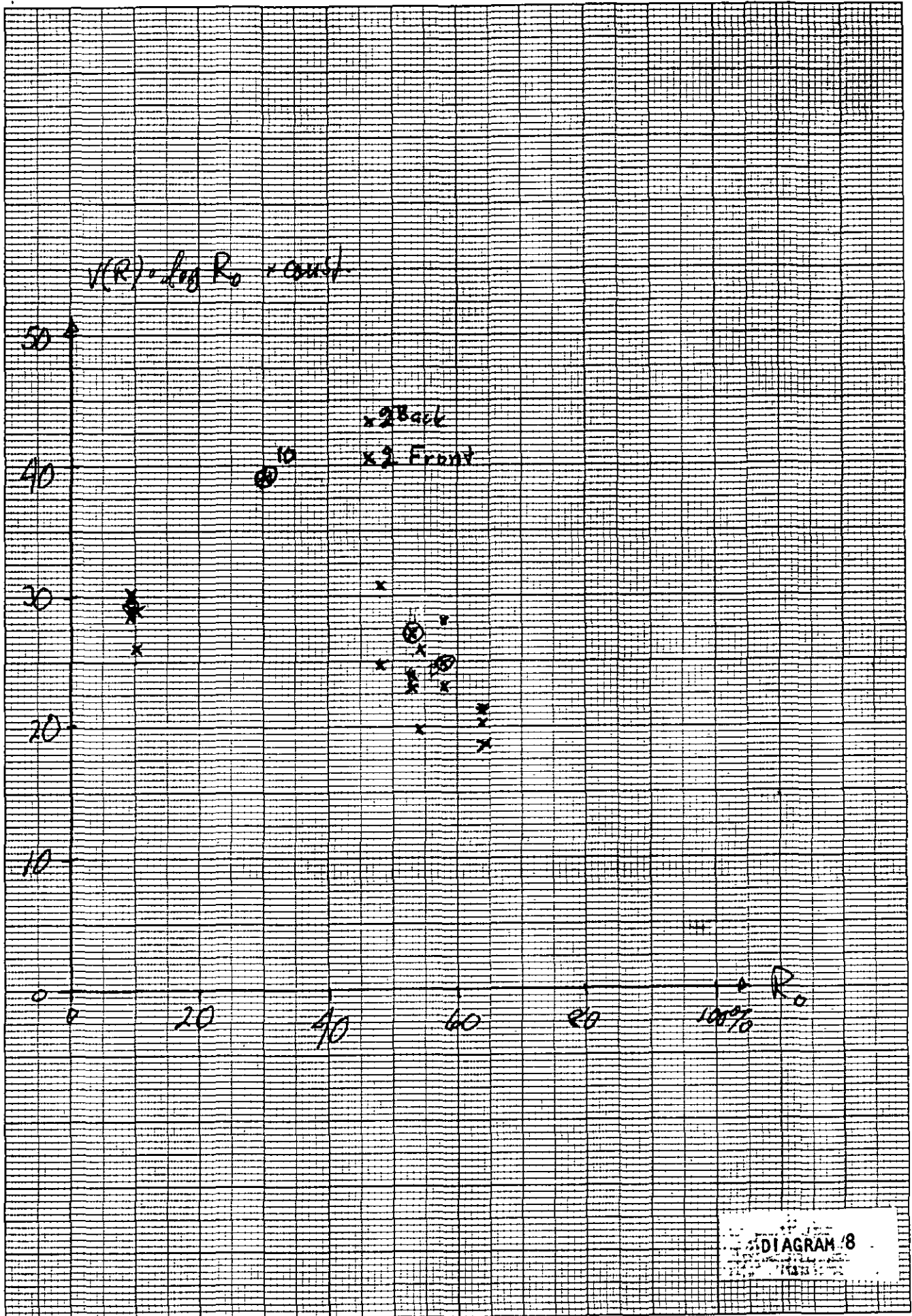


DIAGRAM 8

The human eye and brain respond to light and light intensity variations in a very complex way. The well-known Weber-Fechner's law states that the response is proportional to the logarithm of the light intensity. A simple measure of the "subjective" intensity of light variations would then be the standard deviation, or RMS value, of the logarithm of the light intensity.

$$u_1 = \text{RMS}(\log I)$$

Since the light intensity, I is the product of the incident light intensity, I_0 , and the reflectance, R , of the studied surface, and as the RMS value of the logarithm of a variable is for moderate variations, equal to the coefficient of variation of the variable, the above measure can also be written

$$u_1 = \text{RMS}(\log I) = V(I) = V(R)$$

Thus the logarithmic characteristic of the visual sense leads to the conclusion that the coefficient of variation of reflectivity of a print should be one important "subjective" measure. It has also been extensively used. The statements in the previous section about the influence of the properties of the ink and paper as well as the levels of ink and reflectivity on this parameter are also relevant in this context.

Accordingly, subjective assessments of the evenness of solid prints must be made under very carefully controlled conditions with respect to these parameters. Furthermore, results of subjective assessments obtained under circumstances not approaching the ideal in this respect must be treated with extreme care.

A further step on the way towards a better "subjective" measure of the visual perception of unevenness of "mottled" surfaces was proposed by Olle Andersson (6) in connection with work on the "look-through" of paper. He hypothesized that the visual perception of unevenness of a sheet of paper observed by transmitted light was proportional to the RMS value of the spatial derivative of the logarithm of the light intensity

$$u_2 = \text{RMS} \left[\frac{d(\log I)}{dx} \right]$$

He verified this hypothesis by asking a number of people to judge the unevenness of a series of papers by pair comparisons. A similar expression, the rectified average value of the spatial derivative of the reflectance variations, has been proposed and used by Poulter (7) as a measure for the "mottle" of solid prints.

Since it seems possible that measures such as these may offer advantages in obtaining better "subjective" measures, some further study is required. For this the more elaborate and more tractable expression proposed by Andersson is chosen. Suppose then that the electrical signal e is proportional to the intensity of the reflected light.

$$e = k_1 I = k_1 R I_0$$

We then find that the unevenness given by Andersson's expression becomes

$$u = \text{RMS} \left[\frac{d(\log I)}{dx} \right] = \text{RMS} \left[\frac{d(\log e)}{dx} \right]$$

It is known from the theory of stochastic processes (8) that the RMS value of the derivative of a stochastic signal is closely related to the intensity and micro scale, λ , of the signal, so that the above expression becomes

$$u = \text{RMS}(\log e) / \lambda = V(R) / \lambda$$

It is also stated in the section on the measuring equipment that the size of the measuring aperture determines the position along the wavelength axis of the maximum of the wavelength spectrum of formation of random sheets. This should also be the case, at least approximately, for the reflectance variations from prints on such sheets. In fact the mathematics indicate that the micro scale of the measured spectrum becomes very nearly equal to the diameter of the measuring aperture. The above formula then simplifies to

$$u = \text{RMS}(\log e) / \varnothing = V(R) / \varnothing$$

where \varnothing is the diameter of the measuring aperture. The formula very clearly points to the fact that the size of the measuring aperture is a most important parameter. It also shows, however, that for well-formed sheets, or for prints that have reflectance variations whose structure resembles that of well-formed sheets, the above hypothesis of Andersson, as well as the one proposed by Poulter, should rank the sheets in the same manner as the simpler coefficient of variation of reflected light.

For real sheets the above statement is not necessarily true. Our measurements show that in most commercial sheets the micro scale of both formation and reflectance variations is very often appreciably (often several times) larger than twice the size of our measuring aperture, which has a diameter of 0.1 mm. Hence Andersson's, and probably also Poulter's measures may in some cases grade papers and prints better than the coefficient of variation of reflectance alone.

This can only be so, however, if the size of the measuring aperture is sufficiently small.

In order to obtain more detailed and significant information on the perception of unevenness, attention is called to a paper by J. Merchant (9). He presents the hypothesis that the human visual sense samples the spatial power spectrum of the input image, just as the aural sense samples the temporal power spectrum of the input sound. The justification for his hypothesis is the fact that the sensitivity of the retina (except at the fovea) to form, or pattern, in the input image is very much poorer than is suggested

ed by the corresponding upper cutoff spatial frequency of the retina. This property is characteristic of power-spectrum sensitive devices. In developing his hypothesis he proposes that the human retina samples the spatial average of the luminance function over the studied area as well as sampling certain weighted averages of the spatial power spectrum within this area.

He points out that this method of sampling introduces ambiguities into the perception of the object except when the latter is very simple, e.g. one sharp line. Merchant's hypothesis seems very plausible and it helps to explain, or rather to put words and numbers to, some familiar observations. An observer of a printed surface easily perceives regular disturbances such as wire and felt marks, streaks, etc.

In a wavelength spectrum such disturbances are represented by quite sharp and high peaks at wavelength corresponding to the distance between the disturbances. It is therefore clear that when such peaks occur (and they do) they should be treated separately and be given special weight in any composite figure that is intended to represent the subjective impression of unevenness.

According to the theory of sheet structure by Haglund, Norman and Wahren (10), the wavelength spectrum of formation should have a rather smooth and simple form. This is also observed in practice in well-formed sheets. However, many commercial and laboratory made papers yield wavelength spectra of formation that contain a "hump" in a particular range of wavelength. This hump is not necessarily a maximum, but only a deviation from the smooth and regular appearance of spectra of random sheets. According to Merchant's hypothesis an observer will perceive such variations in a rather vague and unspecified way. If he does not study the object very carefully (using foveal vision) he will only perceive the existence of irregularities of certain sizes. Depending on their geometrical extension he may perceive them as dots, grains, flocs, blobs or clouds, for instance.

Such irregularities may be disturbing when looking through a sheet of paper as well as when judging the evenness of a solid print. Hence such humps in the measured spectra of formation and reflectivity should also be given special weight.*

After having now given special weight to peaks and humps in the wavelength spectra, and having stated that apart from such irregularities the spectra always have approximately the same shape, it only remains to give some weight to the general level of the spectrum stripped of these irregularities. There are reasons to believe that the level of the spectrum should be given fairly little weight. One reason for this is apparent from Merchant's hypothesis. If the spectrum does not contain any humps

and peaks, the observer will perceive nothing but possibly general background noise. If the noise level is within the normal range he will only perceive it as "paper" or possibly "good or poor paper".

An illustration of the above discussion is given below. It is familiar to most papermakers, if not to all printers. It will also provide a second indication that the average spectral level should not be given too much weight. As part of a rebuild and modernisation programme foils were installed on a medium-speed paper machine producing magazine paper. On start-up the sheet had a very streaky appearance. (perception = streaky = bad) It was soon found that the streaks were due to a twisted forming board and maladjustments in the headbox. As these difficulties could not be immediately remedied, the papermakers decided to remove the first two foil boxes immediately following the headbox, substituting three table rolls in their place. The machine then produced saleable paper until the basic cause of the streaks was remedied and the foils put back into service.

Our formation measurements showed that the "streaky" paper produced on start-up after the re-build had a significantly better formation than the one produced with the table rolls in position right after the headbox. However, the "streaky" paper had a "hump" at wavelengths approximately between 2 and 10 cm. This hump was easily perceived by the eye in an otherwise well formed sheet. When the table rolls were replaced the hump was "drowned" in the general noise of the poor formation of the resulting sheet.

The above example serves to show that, within limits, deviations from a regular spectral shape are much more easily perceived as irregularities than the general level of the variations. It also shows that any simple over-all measure, such as the one based on Andersson's hypothesis, may easily lead to erroneous conclusions.

The optical geometry used to obtain the measurements should of course, be similar to that used by an observer. This means that the light should be directional and the measurement should be done using a small spatial angle, for example, a geometry similar to the one described as geometry B in the section on the measuring equipment. This arrangement was chosen here primarily for reasons of convenience. The selected resolution (i.e. the size of the measuring aperture) should be as small as is the least distortion of the signal. When trying to measure one "subjective" figure only, the size of the measuring aperture should probably be related to the resolution of the eye.

* This statement presupposes, of course, that not only the common reader but also paper-makers, printers and advertising people do not normally study the structure of paper and printed surfaces very carefully. For such studies only the complete spectrum will suffice.

Oversized
page

Not copied
Refer to
original.

Oversized
page

Not copied
Refer to
original.

Oversized
page

Not copied
Refer to
original.